Cancer Biol Med 2026. doi: 10.20892/j.issn.2095-3941.2025.0360

ORIGINAL ARTICLE

VDAC1 protein derived from extracellular vesicles promotes paclitaxel resistance in gastric cancer through autophagy and mitophagy

Yanna Bi[1,2*], Sisi Wei[2*], Zhe Zhang[2], Yuqing Wang[2], Yang Wen[2], Hongquan Wang[3], Kexin Li[2], Cong Zhang[2], Yumin Wang[4], Lianmei Zhao[2], Guogui Sun[5]

[1]Department of Clinical Microbiology, North China University of Science and Technology Affiliated Hospital, Tangshan 063000, China; [2]Research Center, The Key Laboratory of Tumor Gene Diagnosis and Treatment, The Fourth Hospital of Hebei Medical University, Shijiazhuang 050011, China; [3]Department of Geriatrics, Aerospace Center Hospital, Peking University Aerospace School of Clinical Medicine, Beijing 100049, China; [4]Department of Respiratory and Critical Care Medicine, Aerospace Center Hospital, Peking University Aerospace School of Clinical Medicine, Beijing 100049, China; [5]Department of Chemoradiation, North China University of Science and Technology Affiliated Hospital, Tangshan 063000, China

ABSTRACT

Objective: Paclitaxel (PTX), a conventional second-line therapeutic agent for advanced gastric cancer (GC), exhibits compromised clinical efficacy due to acquired chemoresistance in patients, the molecular mechanisms of which remain poorly elucidated. This study aimed to investigate the therapeutic potential of targeting extracellular vesicle (EV) protein in reversing PTX resistance in GC cells and to delineate the underlying molecular pathways involved.

Methods: Proteomic profiling was used to identify differentially expressed EV proteins in PTX-resistant GC cells. EVs were isolated *via* size exclusion chromatography (SEC) and characterized using transmission electron microscopy (TEM), nano-flow cytometry (nano-FCM), and western blot analysis. *In vivo* functional validation was performed in xenograft tumor models by injecting EV proteins into nude mice *via* the tail vein (6 groups, $n = 4$). EVs derived from 4,4′-diisothiocyanatostilbene-2,2′-disulfonic acid (DIDS)-treated cells were administered to tumor-bearing nude mouse model (4 groups, $n = 5$) to determine the impact of EV-derived voltage-dependent anion channel protein 1 (VDAC1) on PTX resistance. In addition, VDAC1 protein expression was evaluated using immunohistochemical (IHC) assays in 34 clinical specimens from PTX-resistant patients.

Results: Proteomic analyses demonstrated a marked upregulation of VDAC1 in EVs secreted by PTX-resistant GC cells. Functional studies revealed that intercellular transfer of EV-derived VDAC1 directly conferred PTX resistance to drug-sensitive cancer cells. Gene set enrichment analysis (GSEA) and adenosine triphosphate (ATP) functional assay further elucidated that VDAC1-mediated chemoresistance was mechanistically linked to the activation of adenosine 5′-monophosphate (AMP)-activated protein kinase (AMPK) signaling and concomitant suppression of the mammalian target of rapamycin – p70 ribosomal protein S6 kinase (mTOR-p70S6K) pathway. *In vivo* validation confirmed that systemic delivery of EV-derived VDAC1 significantly reduced PTX sensitivity in GC tumors. Furthermore, DIDS inhibited the expression of the VDAC1 protein in EVs, thereby reducing PTX resistance *in vivo* and *in vitro*. IHC analysis revealed that VDAC1 expression was significantly higher in GC patients with PTX resistance compared to PTX-sensitive patients.

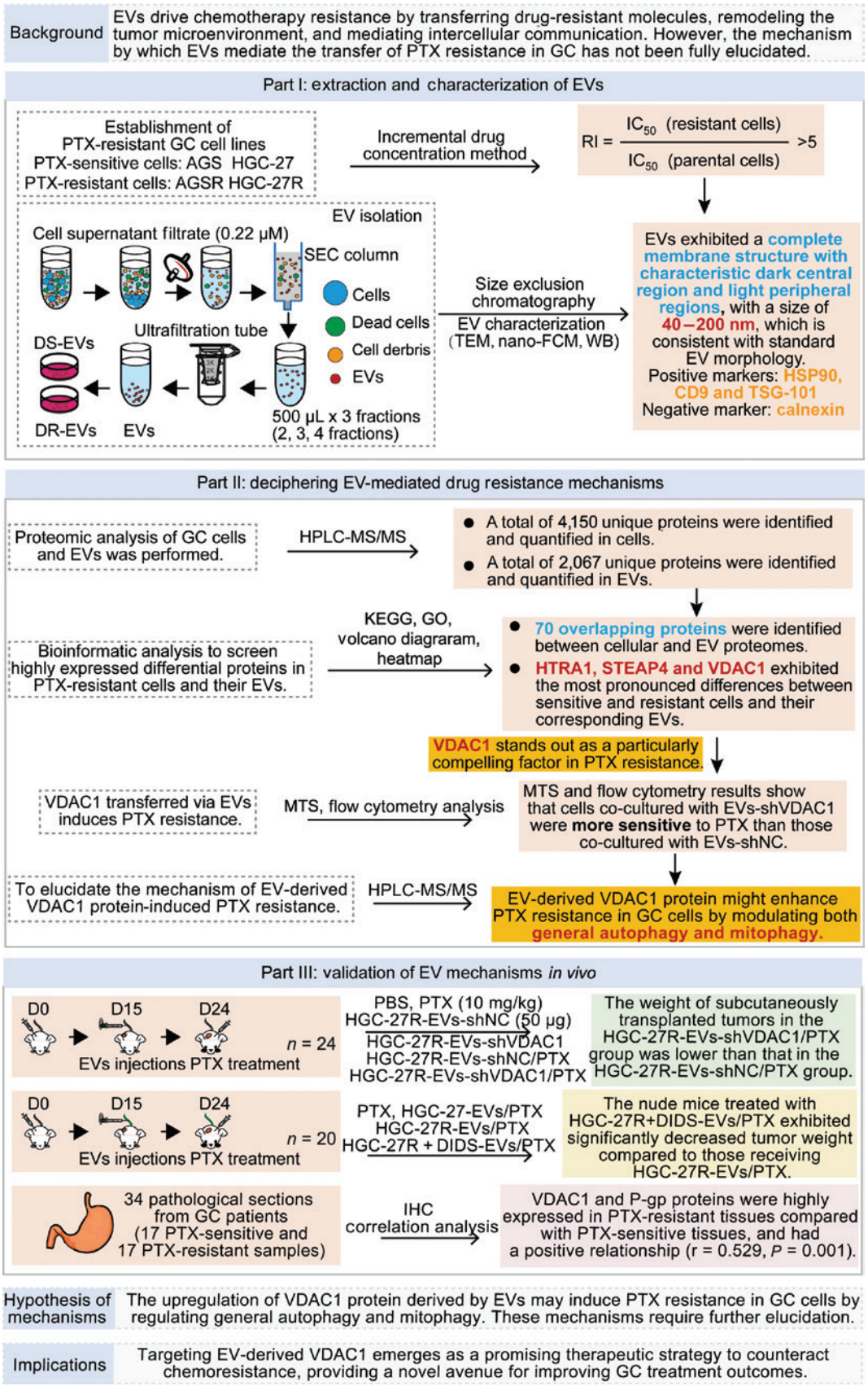
Conclusions: The findings herein underscore the pivotal role of EV-derived VDAC1 in driving PTX resistance in GC through dual modulation of autophagy and mitophagy, mediated by the AMPK/mTOR signaling axis. Targeting EV-derived VDAC1 has emerged as a promising therapeutic strategy to counteract chemoresistance, providing a novel avenue for improving GC treatment outcomes.

KEYWORDS Extracellular vesicles; gastric cancer; paclitaxel-resistance; voltage-dependent anion channel protein 1; autophagy; mitophagy

Introduction

Gastric cancer (GC) ranks as the fifth most prevalent malignant tumor worldwide[1,2]. Chemotherapy remains the cornerstone treatment for metastatic and unresectable GC[3]. Paclitaxel (PTX), an anti-microtubule agent, has demonstrated clinical efficacy both as a monotherapy and in combination regimens for advanced GC[4]. However, acquired chemoresistance significantly limits the clinical efficacy of PTX-based chemotherapy[5]. Accumulating evidence suggests that cancer cell drug resistance

*These authors contributed equally to this work.
Correspondence to: Guogui Sun
E-mail: guogui_sun2021@sina.com
ORCID ID: https://orcid.org/0000-0003-0348-0858
Received July 15, 2025; accepted December 15, 2025;
published online February 17, 2026.
Available at www.cancerbiomed.org
© 2026 The Authors. Creative Commons Attribution-NonCommercial 4.0 International License (CC BY-NC 4.0)


Background
EVs drive chemotherapy resistance by transferring drug-resistant molecules, remodeling the tumor microenvironment, and mediating intercellular communication. However, the mechanism by which EVs mediate the transfer of PTX resistance in GC has not been fully elucidated.
Part I: extraction and characterization of EVs
Establishment of PTX-resistant GC cell lines
PTX-sensitive cells: AGS HGC-27
PTX-resistant cells: AGSR HGC-27R
Incremental drug concentration method
RI = IC50 (resistant cells) / IC50 (parental cells) >5
EV isolation
Cell supernatant filtrate (0.22 μM)
SEC column
Cells
Dead cells
Cell derbris
EVs
Ultrafiltration tube
DS-EVs
DR-EVs
EVs
500 μL x 3 fractions (2, 3, 4 fractions)
Size exclusion chromatography
EV characterization (TEM, nano-FCM, WB)
EVs exhibited a complete membrane structure with characteristic dark central region and light peripheral regions, with a size of 40–200 nm, which is consistent with standard EV morphology.
Positive markers: HSP90, CD9 and TSG-101
Negative marker: calnexin
Part II: deciphering EV-mediated drug resistance mechanisms
Proteomic analysis of GC cells and EVs was performed.
HPLC-MS/MS
A total of 4,150 unique proteins were identified and quantified in cells.
A total of 2,067 unique proteins were identified and quantified in EVs.
Bioinformatic analysis to screen highly expressed differential proteins in PTX-resistant cells and their EVs.
KEGG, GO, volcano diagraram, heatmap
70 overlapping proteins were identified between cellular and EV proteomes.
HTRA1, STEAP4 and VDAC1 exhibited the most pronounced differences between sensitive and resistant cells and their corresponding EVs.
VDAC1 stands out as a particularly compelling factor in PTX resistance.
VDAC1 transferred via EVs induces PTX resistance.
MTS, flow cytometry analysis
MTS and flow cytometry results show that cells co-cultured with EVs-shVDAC1 were more sensitive to PTX than those co-cultured with EVs-shNC.
To elucidate the mechanism of EV-derived VDAC1 protein-induced PTX resistance.
HPLC-MS/MS
EV-derived VDAC1 protein might enhance PTX resistance in GC cells by modulating both general autophagy and mitophagy.
Part III: validation of EV mechanisms in vivo
D0 D15 D24
n = 24
EVs injections PTX treatment
PBS, PTX (10 mg/kg)
HGC-27R-EVs-shNC (50 μg)
HGC-27R-EVs-shVDAC1
HGC-27R-EVs-shNC/PTX
HGC-27R-EVs-shVDAC1/PTX
The weight of subcutaneously transplanted tumors in the HGC-27R-EVs-shVDAC1/PTX group was lower than that in the HGC-27R-EVs-shNC/PTX group.
D0 D15 D24
n = 20
EVs injections PTX treatment
PTX, HGC-27-EVs/PTX
HGC-27R-EVs/PTX
HGC-27R + DIDS-EVs/PTX
The nude mice treated with HGC-27R+DIDS-EVs/PTX exhibited significantly decreased tumor weight compared to those receiving HGC-27R-EVs/PTX.
34 pathological sections from GC patients (17 PTX-sensitive and 17 PTX-resistant samples)
IHC correlation analysis
VDAC1 and P-gp proteins were highly expressed in PTX-resistant tissues compared with PTX-sensitive tissues, and had a positive relationship (r = 0.529, P = 0.001).
Hypothesis of mechanisms
The upregulation of VDAC1 protein derived by EVs may induce PTX resistance in GC cells by regulating general autophagy and mitophagy. These mechanisms require further elucidation.
Implications
Targeting EV-derived VDAC1 emerges as a promising therapeutic strategy to counteract chemoresistance, providing a novel avenue for improving GC treatment outcomes.

Study Flow **Part I** focuses on model establishment, including the development of PTX-resistant GC cell lines and the extraction of EVs from drug-sensitive and -resistant cells. **Part II** emphasizes the correlation between EVs and PTX resistance. EVs secreted by resistant cells confer drug resistance to sensitive cells *via* horizontal protein transfer. Mechanistically, EVs carrying VDAC1 are internalized by sensitive cells, significantly reducing PTX sensitivity by activating general autophagy and mitophagy pathways. **Part III** involves *in vivo* validation and mechanistic exploration. EVs derived from resistant cells systemically transferred PTX resistance in the nude mouse xenograft model. This resistance-inducing capacity was markedly attenuated upon blocking VDAC1 function with the DIDS inhibitor. These findings highlighted the therapeutic potential of targeting EV-derived VDAC1. DIDS, 4,4′-diisothiocyanatostilbene-2,2′-disulfonic acid; DR-EVs, EVs derived from PTX-resistant cells; DS-EVs, EVs derived from PTX-sensitive cells; EV, extracellular vesicle; GC, gastric cancer; IC_{50}, half maximal inhibitory concentration; IHC, immunohistochemistry; nano-FCM, nano-flow cytometry; PTX, paclitaxel; RI, resistance index; TEM, transmission electron microscopy; VDAC1, voltage-dependent anion channel protein 1; WB, Western blot.

is a major contributor to treatment failure, which drives tumor recurrence, disease progression, and ultimately patient death[6]. Notably, GC exhibits higher tissue heterogeneity and invasive potential than other solid malignancies[7]. Therefore, elucidating the mechanisms underlying drug resistance in GC and addressing unmet therapeutic needs are urgently needed.

Extracellular vesicles (EVs), which are small lipid membrane vesicles secreted by almost all cell types, have been shown to transmit molecular information through intercellular transfer (proteins, nucleic acids, and metabolites). EVs are implicated in immune responses, cardiovascular disease, central nervous system disorders, and cancer progression[8,9]. Recent studies have demonstrated that EVs derived from drug-treated cancer cells hinder chemotherapy efficacy and promote chemoresistance through diverse mechanisms[10-12]. EVs transfer non-coding RNAs [e.g., micro (mi)RNA] to recipient cells, which modulates apoptotic pathways, upregulates drug-efflux pumps (e.g., ATP-binding cassette (ABC) and solute carrier (SLC) transporters transporters), and enhances cancer stemness, thereby conferring chemoresistance[13]. Alternatively, surface ligands (e.g., MHC-II) engage receptor-mediated endocytosis/membrane fusion, delivering resistance-associated proteins [e.g., P-glycoprotein (P-gp)] to activate pro-survival signaling and reduce intracellular drug accumulation[14]. These processes establish EVs as key vectors for tumor cells to eliminate resistance factors, remodel the microenvironment, and disseminate resistant phenotypes. While EV-mediated transfer of miRNA and long non-coding (lnc)RNA has been extensively investigated[15-19], the functional role of EV proteins in chemoresistance remains poorly characterized. Therefore, this study aimed to investigate the contribution of specific EV protein cargo isolated from PTX-resistant GC cells to chemotherapeutic resistance development.

The investigation first identified a series of proteins enriched in EVs derived from PTX-resistant GC cells. Voltage-dependent anion channel protein 1 (VDAC1) was identified as a highly abundant protein component in these EVs. Functional analyses demonstrated that EV-mediated intercellular transfer of VDAC1 promoted PTX resistance in both *in vivo* and *in vitro* models. Mechanistic investigations revealed that PTX resistance was primarily mediated by EV-derived VDAC1 through the AMPK/mTOR pathway, which involved activation of general autophagy and mitophagy. Notably, the VDAC1 inhibitor, 4,4′-diisothiocyanatostilbene-2,2′-disulfonic acid (DIDS), was shown to effectively reverse PTX resistance in GC cells. These findings established EV-derived VDAC1 as a critical mediator of PTX resistance and proposed targeting EV-derived VDAC1 as a novel therapeutic strategy to overcome chemoresistance in GC.

Materials and methods

Cell culture

GC cell lines (AGS and HGC-27) were obtained from the Shanghai Institute for Biological Sciences (Shanghai, China) with short tandem repeat certification. All cells were cultured in RPMI-1640 medium (Gibco, Grand Island, NY, USA) supplemented with 10% fetal bovine serum [FBS] (BI, Kibbutz Beit Haemek, Israell) and penicillin and streptomycin (Invitrogen, Carlsbad, CA, USA) and incubated at 37°C in 5% CO_2.

Construction of the PTX-resistant GC cell line

Parental AGS and HGC-27 cells in the logarithmic growth phase were cultured in RPMI-1640 medium supplemented with PTX at an initial concentration of 30 nM. After achieving stable proliferation, the PTX concentration was stepwise increased to 100 nM, 200 nM, and finally 300 nM. Cells demonstrating stable survival at 300 nM PTX were designated as PTX-resistant lines. Prior to experimental use, resistant cells were maintained in PTX-free medium for 2 weeks to eliminate acute drug effects. The resistance index (RI) was calculated as follows: $RI = \frac{IC_{50}\,(\text{resistant cells})}{IC_{50}\,(\text{parental cells})}$.

EV isolation

EVs were isolated from GC cell conditioned media using SEC according to an established protocol[20]. Briefly, SEC columns (Echo9101A-5 mL; Echobiotech, Beijing, China) were pre-equilibrated with 20 mL of 0.01 M PBS. Cell culture supernatants were first filtered through 0.22-μm membranes (SLGPR33RB; Millipore, Billerica, MA, USA) and 1 mL of the filtrate was loaded onto the SEC column. After confirming

complete sample loading (no residual flow-through), EVs were eluted with 0.01 M PBS to separate components by molecular weight. Sequential fractions (500 μL per fraction) were collected with fractions 2–4 pooled into 1.5 mL microcentrifuge tubes and concentrated using 100 kDa Amicon Ultra-15 ultrafiltration devices (UFC810024; Millipore) *via* centrifugation at 3500 × g for 10 min at room temperature. EVs isolated from 1 mL of the supernatant were resuspended in 100 μL of PBS. EV protein concentrations were determined using a BCA kit (23225; Thermo Fisher, Waltham, MA, USA).

Blocking EV biogenesis

Cells were seeded in culture dishes. When cell confluence reached 60%–70%, 20 μM GW4869 (HY-19363; MCE, Lawrenceville, NJ, USA) was added and incubated for 24 h. The cell supernatant was subsequently harvested for EV isolation and analysis.

EV characterization

EVs include exosomes and microvesicles, according to the 2018 Minimal Information for Studies of Extracellular Vesicles (MISEV) guidelines[21].

We analyzed EVs using TEM and nano-FCM according to previously published protocols[20]. Isolated EVs (10 μL) were adsorbed onto formvar-carbon electron microscopy grids for 10 min at room temperature. The grids were then stained with 2% uranyl acetate (pH 7.0) for 1 min, blotted dry with filter paper, and air-dried for 2 min prior to observation under an HT7800 TEM (Hitachi Limited, Tokyo, Japan). Nano-FCM (U30; Nanofcm, Fujian, China) was utilized to analyze particle size distribution and concentration of EV samples following the manufacturer's manual and as referenced in a previous report[22]. EV markers [Cluster of Differentiation 9 (CD9), Heat-shock protein90 (HSP90), Tumor susceptibility gene 101 (TSG-101)] were utilized as positive controls in the western blot analyses. In contrast, the endoplasmic reticulum protein, calnexin, was used as the negative control.

PKH67 staining for EVs

EVs were labeled with the PKH67 Green Fluorescent Cell Linker Kit for General Cell Membrane Labeling (1 μM, MKCN7808; Sigma, St. Louis, MO, USA) following the manufacturer's protocol. Diluent C (970 μL) was used to dilute the EVs, then 4 μL of PKH67 dye was added to 1 mL of Diluent C and incubated for 5 min. FBS (3.8 mL) was subsequently added to terminate the staining. Finally, the labeled EVs were collected by centrifugation in a 100 kDa ultrafiltration tube and co-cultured with the cells for 6 h. Staining was performed using DAPI (#C0065; Solarbrio, Beijing, China), and images were captured using a laser confocal microscope (Ti2-U; Nikon, Tokyo, Japan).

Western blot analysis

Western blots were performed according to the previously published protocol[23]. The primary antibodies used in western blots were as follows: β-actin (1:1000, T002; Affinity, Cincinnati, OH, USA); GAPDH (1:5000, 104941-AP; Proteintech, Wuhan, China); P-gp (1:3000, 22336-1-AP; Proteintech); CD9 (1:1000, sc-13118; Santa Cruz Biotechnology, Inc., Santa Cruz, CA, USA), HSP90 (1:5000, 13171-1-AP; Proteintech); calnexin (1:1000; c-23954; Santa Cruz Biotechnology, Inc. USA); TSG101 (1:1000, c-7964; Santa Cruz Biotechnology, Inc.); VDAC1 (1:1000, PTM-6157; PTM Biolabs, Chicago, IL, USA); p62 (1:1000, #5114; Cell Signaling Technology, Danvers, Massachusetts, USA); LC3B (1:1000, L7543; Sigma); ULK1 (1:1000, 20986-1-AP; Proteintech); p-ULK1 (1:1000, #14202; Cell Signaling Technology); AMPK (1:1000, #5831; Cell Signaling Technology); p-AMPK (1:1000, #2535; Cell Signaling Technology); mTOR (1:5000, 20657-1-AP; Proteintech); p-mTOR (1:2000, 67778-1-Ig; Proteintech); p70S6K (1:2000, 14485-1-AP; Proteintech); p-p70S6K (1:1000, #AF3228; Affinity); ATG5 (1:1000, 10181-2-AP; Proteintech); ATG7 (1:1000, 10088-2-AP; Proteintech); HTRA1 (1:1000, 55011-1-AP, Proteintech); and STEAP4 (1:1000, 11944-1-AP; Proteintech).

Cell proliferation assay

Cells pretreated under specified conditions were harvested and plated in 96-well plates (Corning, NY, USA) at a density of 4000 cells per well. After incubation for 12 h, the indicated concentration of PTX was added to the cultures. Following a 48 h treatment, MTS solution (2 mg/mL, #75-79-6; Sigma) was added to each well and incubated at 37°C for 2 h. Absorbance was measured at 492 nm using a microplate reader (Thermo Multiskan Ascent, Waltham, MA, USA).

Apoptosis assay

Cells were carefully harvested. The cells were subsequently washed twice with PBS, stained with 5 μL of 7-AAD (51-68981E; BD, San Diego, CA, USA) and 5 μL of PE Annexin V (51-65875X; BD) for 15 min, then analyzed using flow cytometry (FACSCalibur; BD).

RNA isolation

RNA isolation and quantitative real-time polymerase chain reaction (qPCR) analysis were performed according to the previously published protocol[23]. The primer sequences are shown in **Table S1**.

Gene knockdown or overexpression

Small interfering (si)RNA (GenePharma, Shanghai, China) or short hair (sh)RNA (Genechem) was transfected for knockdown of VDAC1 (**Table S2**). VDAC1 was inhibited using 0.25 mmol/L DIDS (HY-D0086; MCE). The GFP-microtubule-associated proteins 1A/1B light chain 3B (LC3B) overexpressing plasmid was purchased from Sangon Biotech (Shanghai, China). Co-transfection was performed with Lipofectamine 2000 (Invitrogen) according to the manufacturer's instructions.

Mass spectrometry-based proteome profiling

Proteomics analysis was performed according to the previously published protocol[24].

Autophagosome detection

Autophagosomes were observed in GC cells. The cells were collected and fixed in a 2.5% glutaraldehyde solution following treatment under specified conditions for embedding, sectioning, and observation under a TEM.

Reactive oxygen species (ROS) detection assay

Seed cells into 6-well plates and culture for 24 h. Aspirate the original medium and gently wash the cells once or twice with pre-warmed wash buffer. Add freshly prepared DCFH-DA (Beyotime, Shanghai, China) working solution to each well or each group of cells, then place the plates in a 37°C incubator and incubate in the dark for 30 min. Detect cellular ROS using immunofluorescence microscopy or flow cytometry.

Detection of Adenosine triphosphate (ATP) levels

Intracellular ATP was detected using an ATP assay kit (S0026; Beyotime Biotechnology). Lysis buffer was added to the cells and the supernatant was collected after centrifugation at 12,000 × g for 5 min. Next, 100 μL of supernatant was added to 100 μL of ATP detection solution and the luminescence was measured using an illuminometer (Cytation5, Winooski, VT, USA). Protein concentrations were determined using the Pierce BCA Protein Assay Kit (Rockford, IL, USA).

Measurement of mitochondrial membrane potential (Δψm)

Take an aliquot of cell suspension and add an equal volume of JC-1 working solution (5 μM, HY-K0601; MCE), mixing gently. In a separate cell sample, pretreat with CCCP (final concentration typically 10–50 μM) at 37°C for 5–20 min, then add the JC-1 working solution. Incubate all samples at 37°C in the dark for 15–30 min. Detect Δψm using immunofluorescence microscopy and flow cytometry.

Mitochondrial mass determination

Mitochondrial mass was detected by incubating cells with 100 nM Mito-Tracker Red CMXRos (C1035; Beyotime Biotechnology) in the dark for 30 min. Confocal microscopy (Leica, Wetzlar, Hesse, Germany) was used to visualize the mitochondrial structure.

Co-localization analysis of mitochondria with mitophagy markers

Mitochondrial co-existence with LC3B spots or lysosomes were observed by confocal microscopy or a real-time live-cell imager (Sartorius, Ann Arbor, Michigan, USA). Cells were incubated with 50 nM Lyso-Tracker Red (C1046; Beyotime Biotechnology) and 50 nM Mito-Tracker Green (C1048; Beyotime Biotechnology) for 30 min in the dark, then treated with the indicated concentrations of PTX to detect mitochondrial and lysosomal co-localization.

Cells were mixed with 2 μg of GFP-LC3B (Beyotime Biotechnology) and 100 nM Mito-Tracker Red CMXRos, then treated with the indicated concentrations of PTX to detect mitochondrial and autophagosome co-localization.

In vivo nude mouse xenograft model

Twenty-four male BALB/c nude mice (4 weeks old) were obtained from Beijing HFK Bioscience Co. (Beijing, China). PTX-sensitive HGC-27 tumor cells (2×10^6) were subcutaneously injected into the right flank of nude mice. The nude mice were randomly divided into 6 groups when the tumor volume reached approximately 50 mm^3. EVs were administered *via* tail vein injection every 3 d. PTX was intraperitoneally injected every 3 d for 2 weeks when tumor volumes reached approximately 100 mm^3. Tumor volumes were measured every 3 d and the nude mice were euthanized after 6 weeks for tumor collection.

Twenty male BALB/c nude mice (4 weeks old) were subcutaneously with PTX-sensitive HGC-27 tumor cells (2×10^6) in the right flank of nude mice. The nude mice were then randomly divided into 4 groups according to the treatment regimen: PTX; HGC-27-EVs/PTX; HGC-27R-EVs/PTX; and HGC-27R+DIDS-EVs/PTX. EVs (0.25 mg/mL [200 μL]) were administered *via* tail vein injection every 3 d when the tumor

volume reached approximately 50 mm^3. PTX (10 mg/kg) was injected intraperitoneally every 3 d for 2 weeks when tumor volumes reached 100 mm^3. Tumor volumes were measured every 3 d and nude mice were euthanized after 6 weeks for tumor collection. *In vivo* tracking of DiR-labelled (60017; Biotium, Shanghai, China) EVs was performed using a fluorescent imaging system (NightOWL II LB983; Berthold, Bad Wildbad, Germany) with excitation and emission wavelengths of 748 and 780 nm, respectively. Approval was obtained from the Animal Care Ethics Committee of the Fourth Hospital of Hebei Medical University (Approval No. IACUC-4th Hos Hebmu-). The procedures used in this study adhere to the tenets of the Declaration of Helsinki.

Immunohistochemistry (IHC)

Tumor tissues were formalin-fixed and paraffin-embedded, then sectioned. The tumor tissues were incubated overnight at 4°C in the following IHC stains, then incubated in secondary antibodies: P-gp (1:500); LC3B (1:200); VDAC1 (1:1000); p-ULK1 (1:500); p-mTOR (1:1000); p-p70S6K (1:200); p-AMPK (1:50); cleaved caspase-3 (1:1000, #9664; Cell Signaling Technology); and Ki-67 (1:2000, 27309-1-AP; Proteintech). All sections were visualized with an inverted microscope (Ti2-U; Nikon, Tokyo, Japan). The percentage of stained positive cells (A) was multiplied by the intensity (B: 0, negative; 1, weakly positive; 2, positive; 3, strongly positive). The final score for each slide was calculated as A*B.

Statistical analysis

All experiments were repeated three times and GraphPad Prism 8.0 was used for data analysis. Quantitative data are expressed as the mean ± standard deviation and analyzed using Student's t-test or one-way ANOVA. P values < 0.05 were considered statistically significant and all statistical tests were two-tailed.

Ethical approval

The source of human tissue samples, quantity, and basic grouping information. A total of 34 paraffin-embedded tissue blocks were collected from the Department of Pathology, The Fourth Hospital of Hebei Medical University, including 17 blocks from PTX-sensitive patients and 17 blocks from PTX-resistant patients. The procedures used in this study adhered to the tenets of the Declaration of Helsinki. This study was approved by the Ethics Committee of the Fourth Hospital of Hebei Medical University (Approval No. 2022KY067) and conducted in accordance with the national Measures for Ethical Review of Biomedical Research Involving Human Subjects. Informed consent was signed by all participants and included detailed descriptions of the research purpose, clauses on privacy protection, and the right to withdraw. Patient data were de-identified to ensure confidentiality.

Results

Intercellular transfer of EV proteins confers PTX resistance to sensitive GC cells *in vitro*

PTX-resistant GC cell lines (AGSR and HGC-27R) were established *in vitro* to unveil the mechanism underlying resistance to PTX in GC cells (**Figure S1A**). The half maximal inhibitory concentration (IC_{50}) value of PTX was significantly increased compared to parental cells (RI > 5; **Figure 1A**). Moreover, enhanced expression of drug resistance markers [P-gp, BCL2-related protein A1 (BCL2A1), Excision Repair Cross-Complementation Group 1 (ERCC1), Glutathione S-transferase pi 1 (GSTP1)] was noted in AGSR and HGC-27R cells (**Figures 1B and S1B**), indicating successful construction of PTX-resistant GC cell models. Whether conditioned medium from PTX-resistant GC cells could transfer the resistance phenotype was then investigated. Drug-resistant cell conditioned medium (DR-CM) and drug-sensitive cell conditioned medium (DS-CM) were collected and used to treat parental AGS or HGC-27 cells. DR-CM significantly enhanced the resistance of parental GC cells to PTX in a dose-dependent manner (**Figure 1C**). Thus, we hypothesized that PTX resistance could be transmitted from drug-resistant cells to sensitive cells *via* supernatant-mediated communication.

GW4869, an EV release inhibitor, was subsequently used to block EV generation to test whether EVs contribute to DR-CM-induced PTX resistance in GC cells[25]. GW4869 treatment significantly reduced PTX resistance phenotypes induced by DR-CM compared to cells co-cultured with DR-CM alone (**Figure 1D**), suggesting the crucial role of EVs in promoting PTX resistance. EVs were isolated from PTX-resistant and -sensitive cells following established protocols to examine the contribution of EVs derived from DR-CM to PTX resistance[20]. The structure and size distribution of EVs were characterized by TEM and nano-FCM (**Figure S1C**). The results confirmed that EVs exhibited complete membrane structure with characteristic dark central region and light peripheral regions with the size of 40–200 nm, which is consistent with standard EV morphology (**Figure S1D, E**). Furthermore, EV-specific markers (HSP90, CD9, and TSG-101) were positive, while calnexin was negative (**Figure 1E**), validating successful EV extraction in parental and resistance GC cells. In addition, PKH-67-labeled EVs were rapidly internalized by AGS and HGC-27 cells (**Figure 1F**). Notably, EVs derived from PTX-resistant

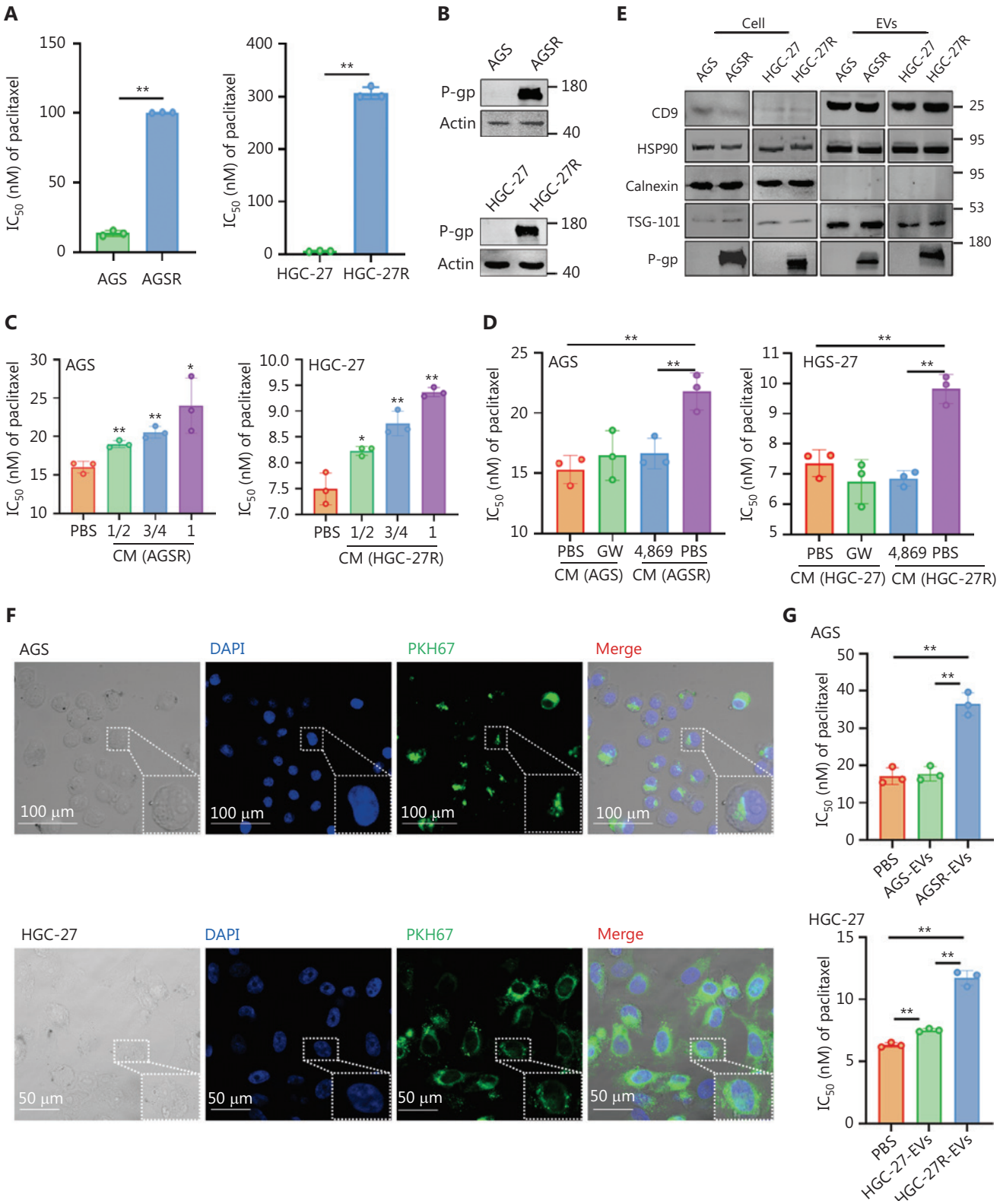


Figure 1 Intercellular transfer of EVs confers PTX resistance to sensitive GC cancer cells *in vitro*. (A) The IC_{50} values of PTX-sensitive (AGS and HGC-27) and -resistant cells (AGSR and HGC-27R) were determined using the MTS assay. (B) The level of P-gp protein expression in PTX-sensitive (AGS and HGC-27) and -resistant (AGSR and HGC-27R) cells was detected by western blot analysis.

Figure 1 (C) The IC_{50} values of PTX-sensitive cells (AGS or HGC-27) pre-cultured with CM from PTX-resistant cells (AGSR-CM or HGC-27R-CM) were determined using the MTS assay. The ratios ("1/2," "3/4," and "1") represent the proportion of AGSR-CM or HGC-27R-CM added to the total culture medium. (D) The IC_{50} values were determined using the MTS assay for PTX-sensitive cells (AGS or HGC-27) pre-cultured with CM of PTX-resistant (AGSR-CM or HGC-27R-CM) cells in the presence of GW4869 (20 μM, 24 h). (E) Western blot analysis of indicated EV markers (CD9, HSP90, calnexin, and TSG-101) in cell lysates and EVs. EV proteins concentrations were determined using a BCA kit. (F) Internalization of AGSR- or HGC-27R-derived EVs containing GFP tags (AGS-EVs or HGC-27-EVs) co-cultured with PTX-sensitive cells (AGS or HGC-27) was determined using confocal microscopy. (G) The IC_{50} values of DR-EVs (AGSR-EVs and HGC-27R-EVs) or DS-EVs (AGS-EVs and HGC-27-EVs) co-cultured with PTX-sensitive cells (AGS and HGC-27) were determined using the MTS assay. *P < 0.05, **P < 0.01. CM, conditioned medium; CD9, Cluster of Differentiation 9; DR-EVs, EVs derived from PTX-resistant cells; DS-EVs, EVs derived from PTX-sensitive cells; EV, extracellular vesicle; GC, gastric cancer; HSP90, Heat-shock protein90; IC_{50}, half maximal inhibitory concentration; PTX, paclitaxel; P-gp, P-glycoprotein; TSG-101,Tumor susceptibility gene 101.

cells (DR-EVs) significantly enhanced PTX resistance in two GC cell lines compared to EVs from PTX-sensitive cells (DS-EVs; **Figure 1G**). Collectively, these data validated the hypothesis that DR-EVs facilitate drug resistance and that the resistance to PTX could be transmitted from drug-resistant cells to sensitive cells.

Proteomic landscapes were established in EVs derived from PTX-resistant cells

A proteomic analysis of GC cells and EVs was performed using HPLC-MS/MS to characterize the specific component within EVs that mediates drug resistance (**Figure 2A**). A total of 4150 unique proteins were identified and quantified in cells with 805 proteins showing significant changes (|fold change| ≥ 1.5; P value ≤ 0.05) in abundance between AGS and AGSR cells (**Figure 2B**). A total of 2067 proteins were detected in EV, including 354 differentially expressed proteins (|fold change| ≥ 1.5; P value ≤ 0.05) in abundance between AGS-EVs and AGSR-EVs (**Figure 2B**). Among these findings, 70 overlapping proteins were identified between cellular and EV proteomes (**Figure 2C**) with expression patterns visualized in **Figure 2D**. Furthermore, KEGG and GO analyses revealed significant enrichment of pathways associated with tumorigenesis, progression, and chemoresistance (**Figures 2E and S1F**).

The top 10 differentially expressed proteins were illustrated next to further probe key mediators of EV-induced PTX resistance, as shown in **Figure 2F**. Among these proteins, HtrA serine peptidase 1 (HTRA1), Six Transmembrane Epithelial Antigen of Prostate 4 (STEAP4), and VDAC1 exhibited the most pronounced differences between sensitive and resistant cells and the corresponding EVs. Then, these proteins underwent western blot analysis and the results manifested significantly elevated expression of HTRA1, STEAP4, and VDAC1 in PTX-resistant cells and DR-EVs (**Figure 2G**). The GEO and DRESIS databases were further screened for PTX resistance-related proteins and prior evidence implicating VDAC1 in PTX resistance across multiple tumor types[26-29]. VDAC1, a predominant β-barrel protein in the mitochondrial outer membrane, was critically implicated in regulating metabolic flux and mitochondrially induced apoptosis by facilitating the release of apoptogenic factors, such as cytochrome c[30,31]. Research on VDAC1 in the context of PTX resistance stems from its essential role in mediating PTX-induced apoptosis. Specifically, PTX triggers the hierarchical activation of activating Transcription Factor 2 (ATF2), which upregulates Bim expression and promotes VDAC1-dependent Bax translocation and cytochrome c release[28]. Inhibition of VDAC1 function, as occurs *via* oligomerization blockade using DIDS, confers profound resistance to PTX by impairing mitochondrial apoptotic signaling, even in the presence of Bcl-2 inhibitors, like ABT-737[32]. Consequently, VDAC1 oligomerization, identified as a druggable target through structural analyses and interactions with anti-apoptotic proteins, represents a pivotal mechanism underlying chemoresistance. Targeting these pathways provides promising therapeutic strategies to overcome PTX resistance in cancer. Therefore, VDAC1 was prioritized for investigation, whereas STEAP4 and HTRA1 showed non-significant effects in subsequent experimental evaluations. Taken together, some proteins in EVs secreted by PTX-resistant cells might contribute to drug resistance in GC cells. Among these proteins, VDAC1 stands out as a particularly compelling factor in PTX resistance.

VDAC1 transferred via EVs induces PTX resistance

siRNAs were used to silence the expression of VDAC1 protein in GC cells to further investigate the potential role of EV-derived VDAC1 protein in mediating intercellular drug resistance transmission. P-gp, an efflux transporter, actively pumps out PTX as a substrate through an ATP-dependent mechanism, thereby mediating multidrug resistance and compromising the antitumor efficacy of PTX[33,34]. Therefore, P-gp protein expression was determined in VDAC1-knockdown drug-resistant cells. Downregulation of VDAC1 in PTX-resistant cells reduced P-gp levels (**Figure 3A**) and significantly

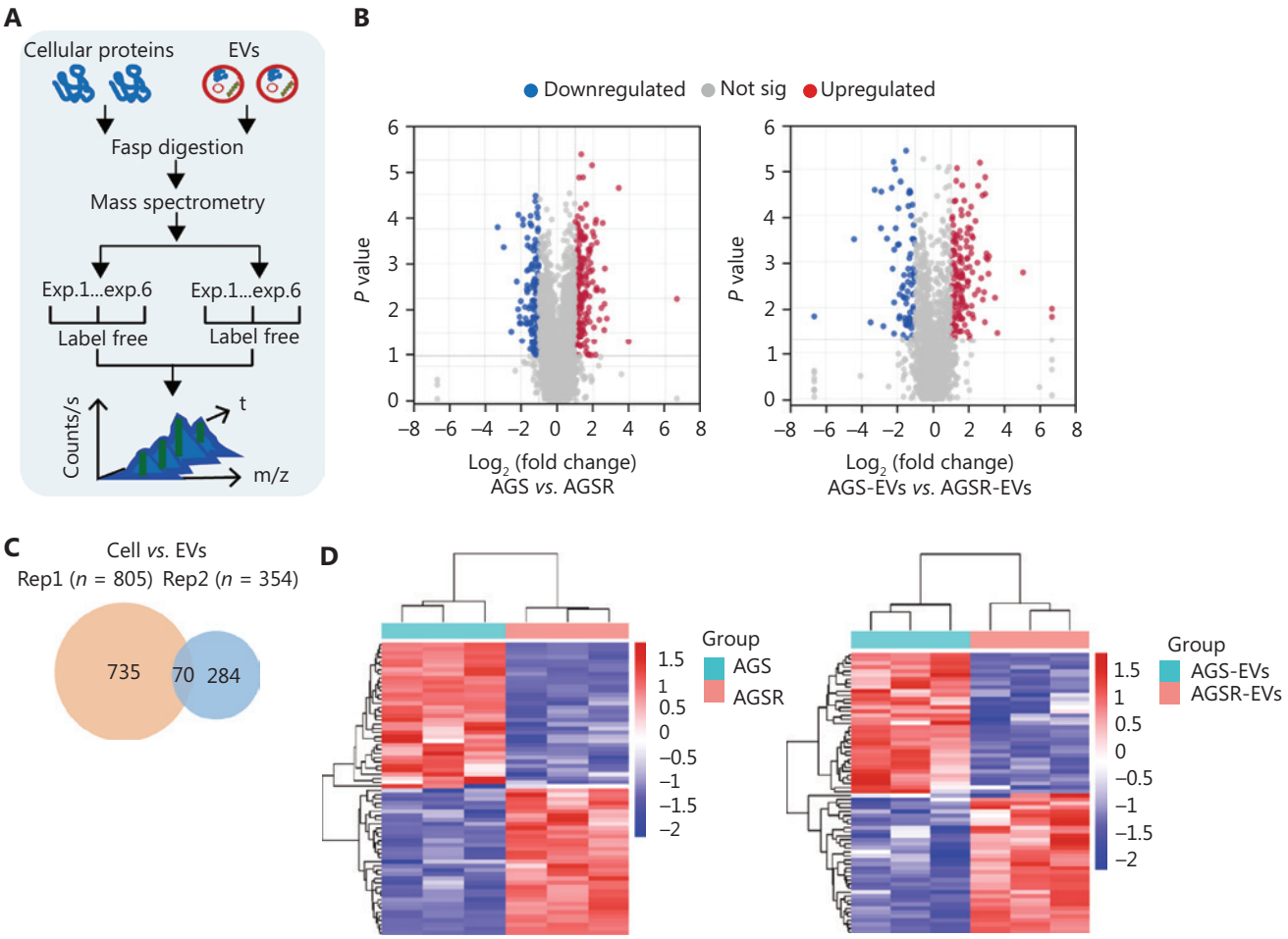


Figure 2 Continued

enhanced PTX sensitivity (**Figure 3B**). However, no such effect was noted upon VDAC1 knockdown in PTX-sensitive cells (**Figure S1G**). Lentivirus-mediated stable VDAC1 knockdown cell lines were subsequently established (**Figure S1H**), from which EVs (EVs-shNC and EVs-shVDAC1) were isolated. As anticipated, EVs derived from VDAC1-deficient cells exhibited markedly reduced VDAC1 and P-gp levels compared to control EVs (**Figure 3C**), suggesting a critical association between EV-derived VDAC1 protein and chemoresistance acquisition. Hence, EVs-shVDAC1 or EVs-shNC were co-cultured with PTX-sensitive GC cells, the results of which showed that cells co-cultured with EVs-shVDAC1 were more sensitive to PTX than those co-cultured with EVs-shNC, suggesting that VDAC1 deficiency leads to decreased ability of EVs to spread resistance (**Figure 3D**). In addition, flow cytometry analysis further revealed increased apoptosis rates in PTX-treated cells exposed to EVs-shVDAC1 *versus* EVs-shNC controls (**Figure 3E**). These findings demonstrated that the EV-derived VDAC1 protein has a crucial role in mediating the transmission of drug resistance among PTX-sensitive cells. Collectively, the results strongly suggested that downregulation of EV-derived VDAC1 protein in GC cells significantly promoted cell sensitivity to PTX treatment and partly overcame EVs-induced PTX resistance.

EV-derived VDAC1 protein enhances autophagic activity in the PTX resistance process

HPLC-MS/MS analysis was performed to analyze the changed proteins in VDAC1 knockdown cells to further elucidate the mechanism underlying EV-derived VDAC1 protein-induced PTX resistance (**Figure 4A**). KEGG analysis revealed that general autophagy and mitophagy pathways were significantly enriched in AGSR upon VDAC1 knockdown (**Figure 4B**). As previously reported, general autophagy and mitophagy are known to mediate tumor cell resistance to chemotherapy[35,36]. Therefore, the hypothesis that VDAC1 promotes PTX

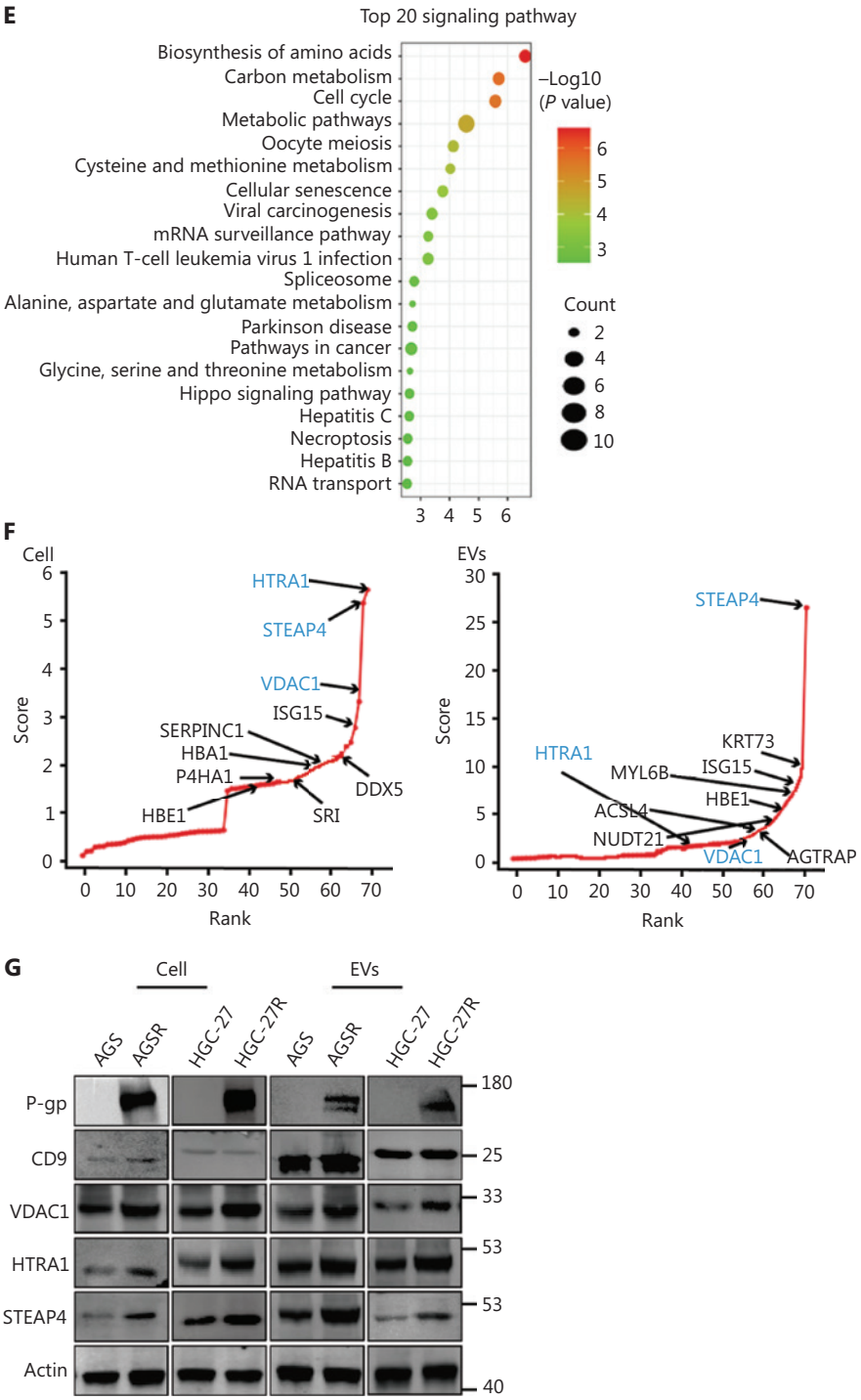


Figure 2 Proteomic landscapes were established in EVs derived from PTX-resistant cells. (A) Schematic diagram of the proteomics design. (B) Volcano diagram analysis of differentially expressed proteins in PTX-sensitive (AGS) and -resistant cells (AGSR) and the secreted EVs (AGS-EVs or AGSR-EVs). (C) Venn diagram analysis of the differentially expressed proteins between the cell (AGSR) and the secreted EVs (AGSR-EVs). (D) Heatmap analysis of the overlapping proteins in cells (AGSR) and EVs (AGSR-EVs). (E) KEGG analysis of overlapped proteins in cells (AGSR) and EVs (AGSR-EVs). (F) The expression trends of the top 10 overlapping proteins in cells (AGSR) and EVs (AGSR-EVs) were analyzed using scatter plots. (G) The levels of VDAC1, HTRA1, and STEAP4 expression in cells (AGSR and HGC-27R) and EVs (AGSR-EVs and HGC-27R-EVs) were detected by western blot analysis. EV, extracellular vesicle; HTRA1, HtrA serine peptidase 1; PTX, paclitaxel; STEAP4, Six Transmembrane Epithelial Antigen of Prostate 4; VDAC1,voltage-dependent anion channel protein 1.

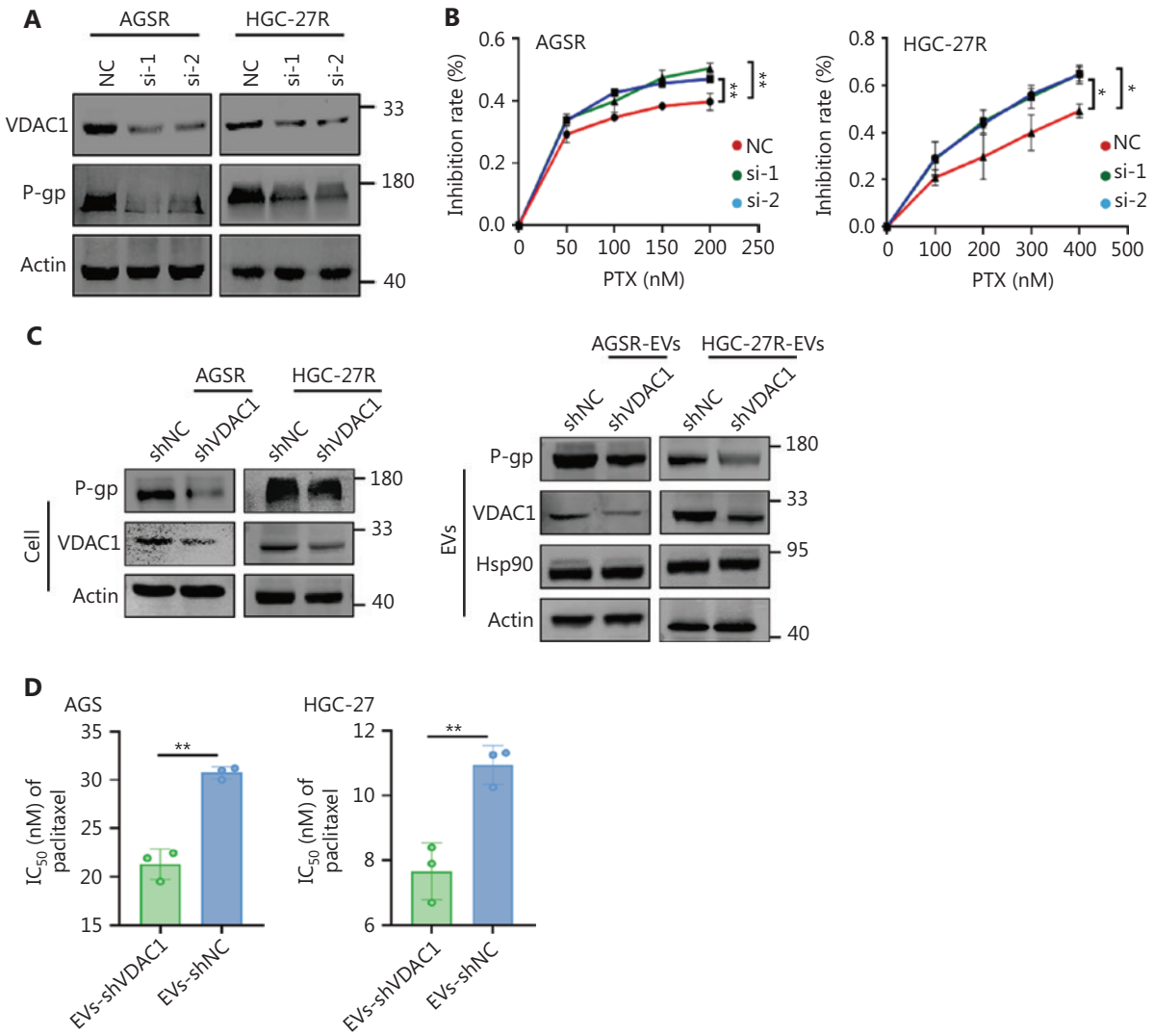


Figure 3 Continued

resistance by modulating general autophagy and mitophagy functions was tested.

First, autophagy levels in PTX-resistant cells were detected. Elevated LC3B-II/I ratios and increased expression of autophagy related 5 (ATG5) and autophagy related 7 (ATG7) were observed in PTX-resistant cells compared to parental cells accompanied by reduced p62 levels (**Figure 4C**). Concurrently, enhanced endogenous LC3B puncta formation was observed in PTX-treated cells with higher levels observed in PTX-resistant counterparts (**Figure 4D**). These results suggested that the enhanced autophagy levels were associated with the acquisition of PTX resistance. Autophagy levels in AGSR cells were measured by silencing VDAC1 to confirm whether alterations in autophagy levels were mediated through VDAC1. Remarkably, elevated LC3B-II/I ratios and increased p62 levels were observed in VDAC1 knockdown AGSR cells compared to the control group (**Figure 4E**). In addition, the transition from autophagosomes to autolysosomes was visualized, and alterations in autophagic flux were assessed in cells, based on the quenching of GFP fluorescence within acidic compartments[37]. The double-tagged mRFP-eGFP-LC3B plasmid was utilized to monitor altered autophagolysosomes. Herein, silencing VDAC1 was shown to increase the quantity of yellow spots (autophagosomes) and reduce the quantity of red spots (autophagolysosomes) in AGSR cells (**Figure 4F**), indicating that VDAC1 knockdown impaired autophagosome-lysosome fusion.

Mitochondrial morphology was assessed using a living cell imager and confocal laser scanning microscope to characterize the mitochondrial alterations in response to PTX treatment in GC cells (**Figure S2A, B**). PTX treatment induced mitochondrial membrane rupture and cristae structure reduction. Flow

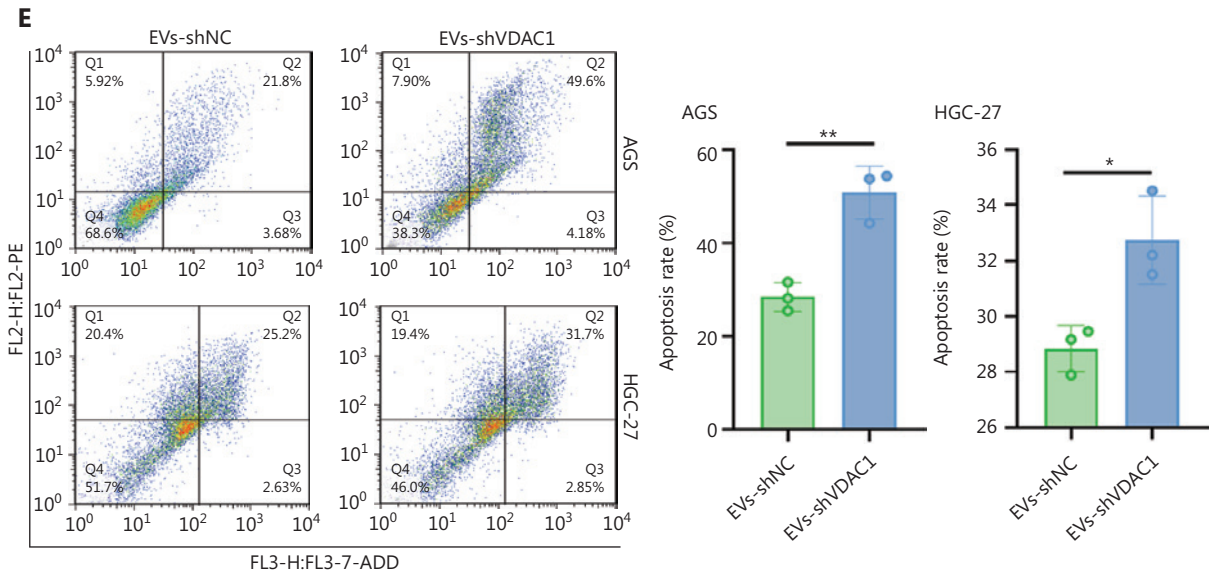


Figure 3 VDAC1 transferred *via* EVs induces PTX resistance. (A) Western blot was used to analyze the levels of P-gp and VDAC1 protein expression in AGSR and HGC-27R cells following VDAC1 knockdown. (B) AGSR and HGC-27R cell inhibition with or without VDAC1 knockdown was measured under PTX treatment. (C) Western blot analysis was performed for VDAC1 and P-gp after infection with lentivirus expressing VDAC1-specific shRNAs in cells (AGSR and HGC-27R) and EVs (AGSR-EVs and HGC-27R-EVs). (D) The IC_{50} values of PTX-sensitive cells (AGS or HGC-27) were determined after pre-cultured with EVs-shNC or EVs-shVDAC1 for 36 h following PTX treatment for another 48 h. (E) Flow cytometry was used to detect apoptosis in PTX-sensitive cells (AGS or HGC-27) pre-cultured with EVs-shNC or EVs-shVDAC1 for 36 h following PTX treatment for another 48 h. EV, extracellular vesicle; IC_{50}, half maximal inhibitory concentration; PTX, paclitaxel; P-gp, P-glycoprotein; VDAC1,voltage-dependent anion channel protein 1.

cytometry analysis demonstrated that ROS levels were significantly elevated in PTX-stimulated GC cells (**Figure S2C**), providing further evidence that PTX treatment induced mitochondrial damage. Mitochondrial damage triggers intracellular surveillance mechanisms that promote encapsulation of impaired mitochondria by autophagosomes[37]. Co-localization of GFP-LC3B-labelled autophagosomes was analyzed with MitoTracker red-labeled mitochondria to investigate the initiation of mitophagy. Enhancement of co-localization between mitochondrial fragments and autophagosomes was observed in AGSR cells treated with high concentrations of PTX compared to controls (**Figure S2D**). Whether PTX regulated mitochondrial transport and mitochondrial degradation processes in lysosomes was further investigate. Notably, increased co-localization of fragmented mitochondria (MitoTracker green) and lysosomes (LysoTracker red) in AGSR cells treated with high concentrations of PTX was noted (**Figure S2E**). Collectively, these results suggested that PTX induces mitophagy in AGSR cells. VDAC1 was knocked down in AGSR cells to further confirm the involvement of VDAC1 in mitophagy. A significant reduction in the co-localization of mitochondria and autolysosomes in VDAC1-knockdown cells was demonstrated, suggesting that VDAC1 regulates mitophagy in PTX-resistant cells (**Figure S2F**). In addition, flow cytometry analysis showed that knockdown of VDAC1 led to increased ROS levels in PTX-resistant cells (**Figure S2G**). The JC-1 probe was used to assess Δψm given that Δψm can initiate mitophagy[38,39]. JC-1 is a potential-sensitive dual-emission dye that exhibits green fluorescence as a monomer under low Δψm conditions, while aggregating into red-fluorescent J-aggregates in functional mitochondria with high Δψm. Knockdown of VDAC1 led to a significant decrease in red fluorescence intensity and an increase in green fluorescence intensity within mitochondria, thereby confirming the critical role of VDAC1 in maintaining Δψm (**Figure S2H, I**). In summary, VDAC1 protein promotes PTX resistance by regulating mitophagy.

In addition, an elevated LC3B-II/I ratio and increased P-gp expression were observed in EVs-shNC-pretreated AGS cells compared to EVs-shVDAC1-pretreated cells; this trend was partially attenuated when the VDAC1 protein level in EVs was reduced (**Figure 4G**). Furthermore, TEM analysis revealed that the quantity of autophagosomes was significantly increased in AGSR cells compared to AGS cells. A similar increase in autophagosome quantity was detected in AGS cells following pretreatment with AGSR-derived EVs. This change in the quantity of autophagosomes was overcome in cells pretreated with EVs-shVDAC1 (**Figure 4H**). Taken together, these findings suggest that EV-derived VDAC1 protein might enhance PTX resistance in GC cells by modulating general autophagy and mitophagy, an effect that is attenuated when EV-derived VDAC1 levels are decreased.

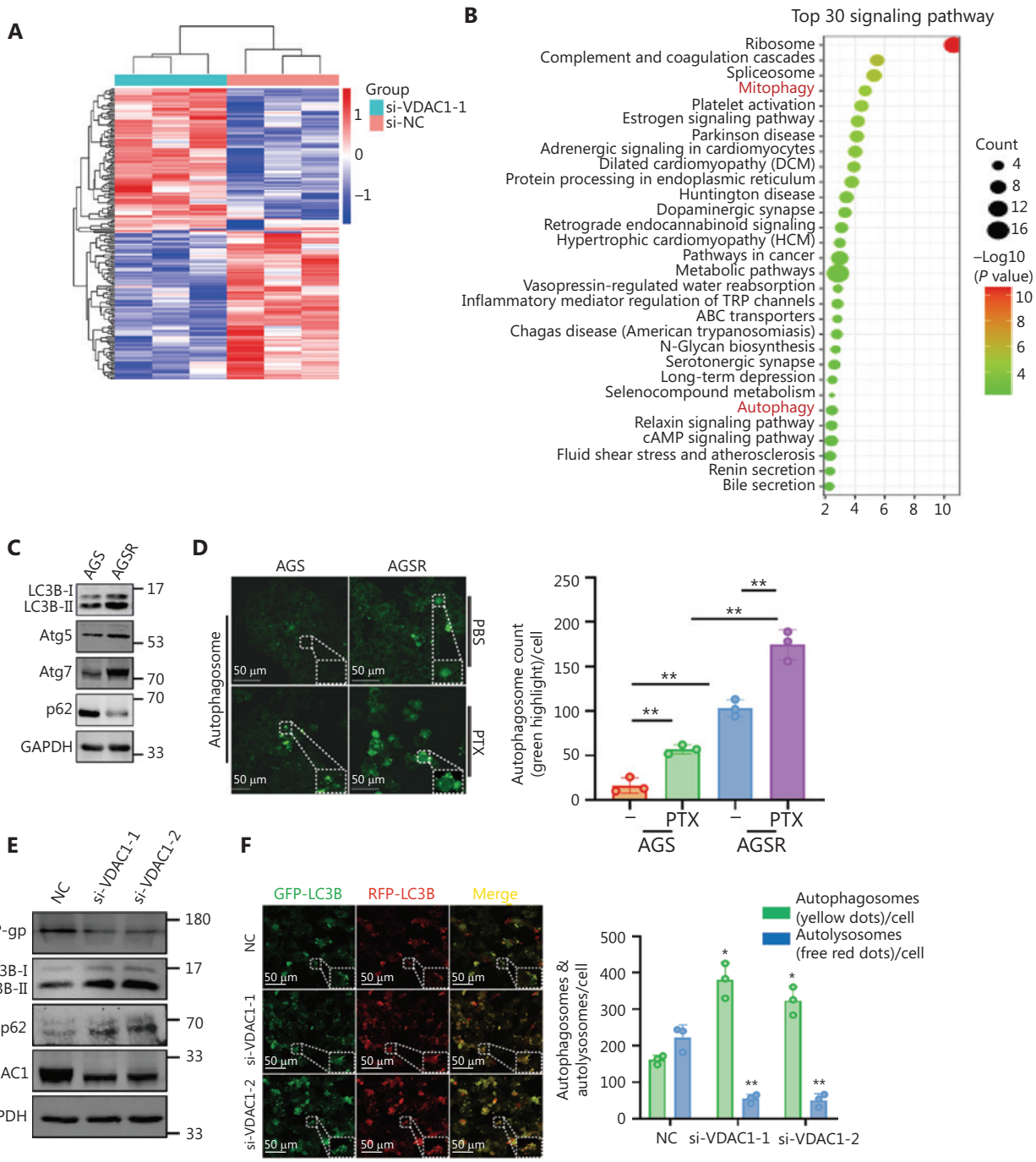


Figure 4 Continued

EV-derived VDAC1 protein activates autophagy by modulating AMPK/mTOR/p70S6K signaling to spread PTX resistance of GC cells

Intracellular ATP levels were measured to further explore the specific pathways through which VDAC1 regulates autophagy. The results demonstrated that net ATP production increased in VDAC1-overexpressing cells compared to control cells, while ATP production was decreased in VDAC1-knockdown cells (**Figure 5A**). Studies have shown that AMPK is the critical cellular energy sensor[40-42]. Therefore, we hypothesized that AMPK is involved in VDAC1-mediated regulation of functions, including autophagy. Furthermore, mass spectrometry

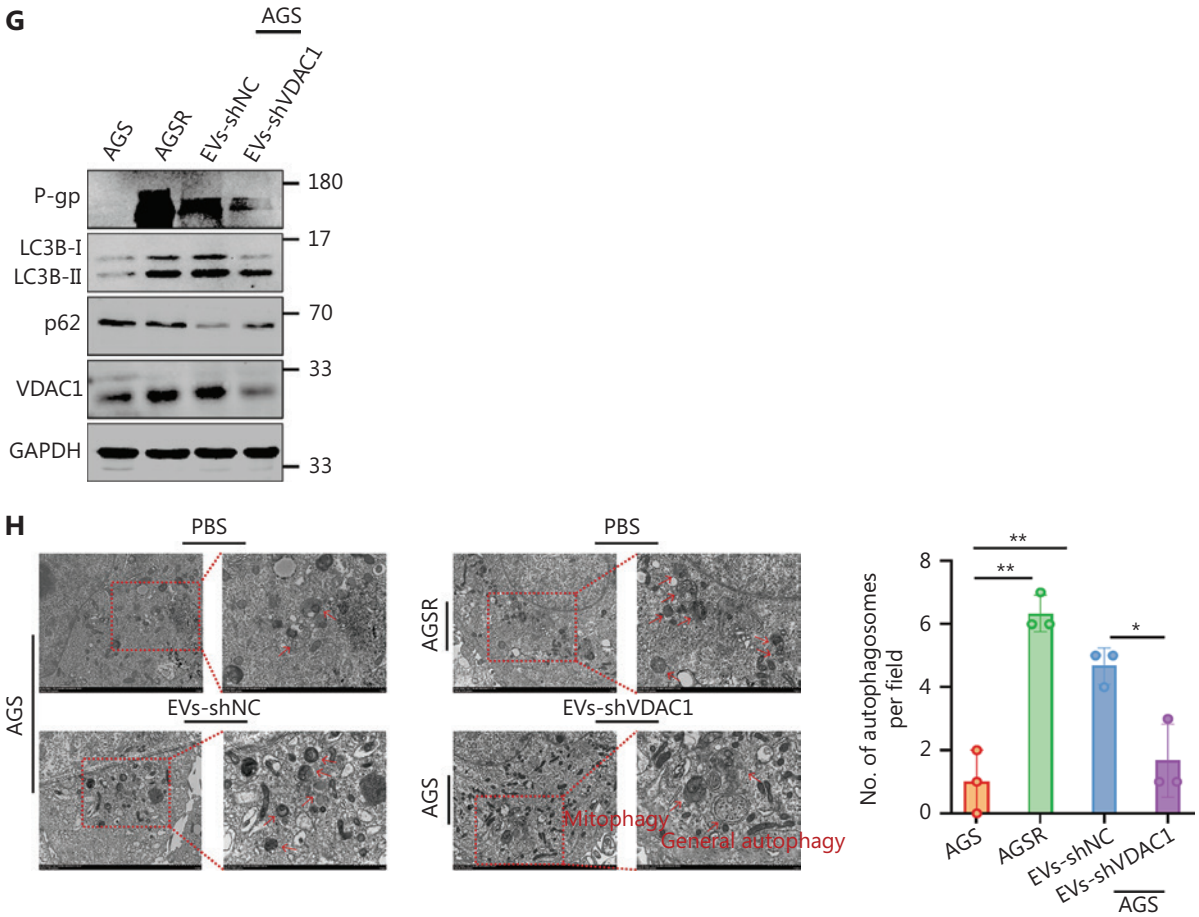


Figure 4 EV-derived VDAC1 protein enhances autophagic activity in the PTX resistance process. (A) Heatmap analysis of differentially expressed proteins in AGSR cells with or without VDAC1 knockdown. (B) The KEGG enrichment analysis was conducted on the top 30 pathways following VDAC1 knockdown in PTX-resistant cells (AGSR). (C) Western blot analysis of ATG5, ATG7, p62, and LC3B-II/LC3B-I in AGS and AGSR cells. (D) Immunofluorescence analysis of endogenous LC3B puncta in AGS and AGSR cells with or without PTX treatment. (E) Western blot analysis of LC3B and p62 in AGSR cells with or without VDAC1 knockdown. (F) Confocal fluorescence microscopy analysis of the quantity of yellow spots (autophagosomes) and red spots (autolysosomes) in AGSR cells with or without VDAC1 knockdown. (G) Western blot analysis of LC3B, p62, and P-gp protein levels in AGS cells after pre-incubation with EVs-shNC or EVs-shVDAC1. (H) TEM analysis of autophagosomes in AGS cells after pre-incubation with EVs-shNC or EVs-shVDAC1. ATG5, Autophagy related 5; ATG7, Autophagy related 7; EV, extracellular vesicle; PTX, paclitaxel; P-gp, P-glycoprotein; TEM, Transmission electron microscopy; VDAC1, voltage-dependent anion channel protein 1.

data obtained after VDAC1 knockdown was utilized to perform GSEA. VDAC1 expression exhibited a negative correlation with the mTOR signaling pathway (**Figure 5B**). These findings support the hypothesis that the AMPK/mTOR autophagy pathway is involved in PTX resistance mediated by EV-derived VDAC1 protein. Moreover, enhanced phosphorylation of AMPK and unc-51 like autophagy activating kinase 1 (ULK1), along with reduced p-p70S6K and p-mTOR levels, were observed in PTX-resistant cells compared to PTX-sensitive cells (**Figure 5C**). Furthermore, VDAC1 knockdown was shown to inhibit AMPK activity and activate the downstream mTOR-p70S6K signaling pathway (**Figure 5D**). These molecular changes suggested that AMPK pathway activation contributes to PTX resistance in GC cells and may be regulated by VDAC1. The mTOR inhibitor, rapamycin (Rapa), was used to further elucidate VDAC1-mediated modulation of the AMPK/mTOR pathway. Rapa partially restored AMPK pathway activity, which was suppressed by VDAC1 knockdown in AGSR cells (**Figure 5E**). These findings suggest that VDAC1 protein promotes autophagy *via* regulation of the AMPK/mTOR pathway, potentially driving the development of PTX resistance in GC cells.

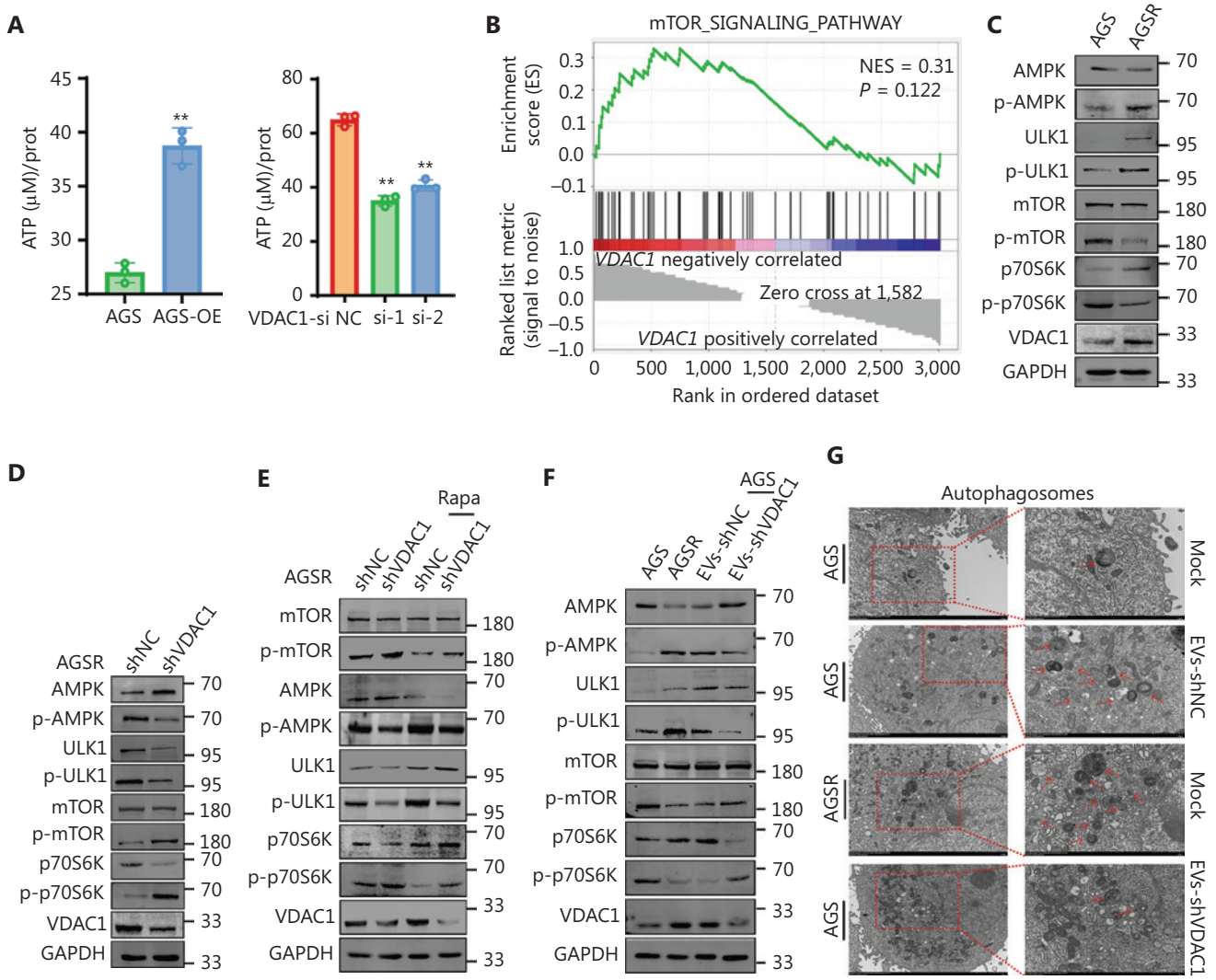


Figure 5 EV-derived VDAC1 protein activates autophagy by modulating AMPK/mTOR/p70S6K signaling to promote the PTX resistance of GC cells. (A) Intracellular ATP levels were measured following VDAC1 overexpression in PTX-sensitive cells (AGS-OE) and VDAC1 knockdown in PTX-resistant cells (AGSR). (B) GSEA analysis of VDAC1 knockdown in PTX-resistant cells (AGSR). (C) Western blot analysis of p-AMPK, p-p70S6K, p-mTOR, and p-ULK1 in AGS and AGSR cells. (D) Western blot analysis of p-AMPK, p-p70S6K, p-ULK1, and p-mTOR in AGSR cells with or without VDAC1 knockdown. (E) Western blot analysis of p-AMPK, p-p70S6K, p-ULK1, and p-mTOR in AGSR cells with or without VDAC1 knockdown in the presence of Rapa (100 nM). (F) Western blot analysis of p-AMPK, p-ULK1, p-mTOR, and p-p70S6K in AGS cells after pre-incubation with EVs-shNC or EVs-shVDAC1. (G) TEM analysis of autophagosomes in AGS cells after pre-incubation with EVs-shNC or EVs-shVDAC1. AMPK, Adenosine 5′-monophosphate (AMP)-activated protein kinase; EV, extracellular vesicle; mTOR, mammalian target of Rapamycin; p70S6K, p70 ribosomal protein S6 kinase; PTX, paclitaxel; Rapa, Rapamycin; TEM, transmission electron microscopy; ULK1, unc-51 like autophagy activating kinase 1; VDAC1, Voltage-dependent anion channel protein 1.

To further investigate the role of EV-derived VDAC1 protein in modulating the AMPK/mTOR signaling pathway through intercellular transfer, the activity of this pathway was assessed in AGS cells incubated with EVs derived from AGSR cells with or without VDAC1 knockdown. As anticipated, elevated AMPK and ULK1 phosphorylation levels, along with reduced p-p70S6K and p-mTOR expression, were observed in AGS cells pre-incubated with EVs-shNC from AGSR cells, mirroring the pathway activity in AGSR cells. However, these effects were partially reversed when cells were treated with EVs derived from VDAC1-knockdown AGSR cells (**Figure 5F**). These findings suggested that EV-derived VDAC1 protein has a critical role in activating the AMPK/mTOR pathway and conferring PTX resistance. Similarly, TME imaging showed a significant

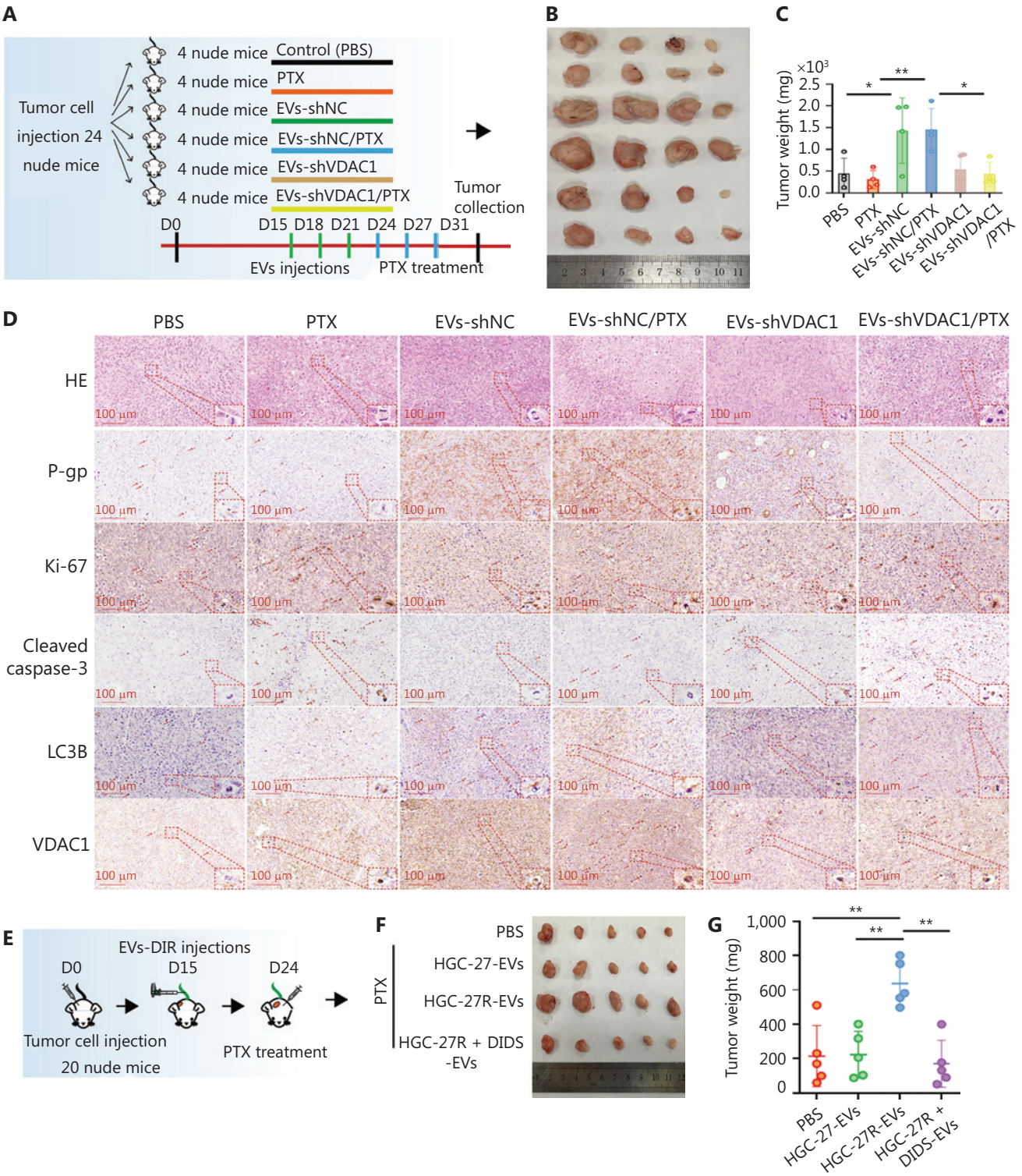


Figure 6 Continued

increase in general autophagy and mitophagy in AGS cells stimulated with EVs-shNC derived from AGSR cells compared to EVs-shVDAC1 (**Figures 5G and S3A**). Collectively, these results indicated that EV-derived VDAC1 protein promoted PTX resistance in GC cells by regulating the AMPK/mTOR/p70S6K signaling pathway.

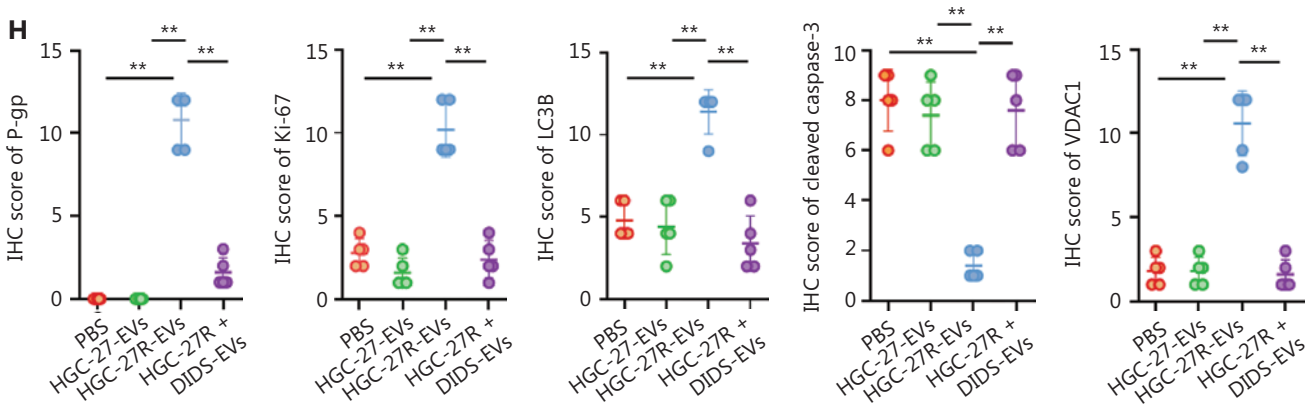


Figure 6 Intercellular transfer of EV-derived VDAC1 protein confers PTX resistance *in vivo*. (A) Schematic diagram of combined treatment with EVs and PTX *in vivo* (n = 24). (B) Schematic representation of tumors in nude mice treated under different conditions (PBS, PTX [10 mg/kg], EVs-shNC [0.25 mg/mL {200 μL}], EVs-shVDAC1 [0.25 mg/mL {200 μL}], EVs-shNC/PTX [0.25 mg/mL {200 μL, 10 mg/kg}], and EVs-shVDAC1/PTX [0.25 mg/mL {200 μL, 10 mg/kg}]). (C) The weight of subcutaneously transplanted tumors in six groups. (D) IHC analysis of cleaved caspase-3, Ki-67, LC3B, VDAC1, and P-gp in subcutaneous transplanted tumors from six groups. (E) Diagram of EVs combined with PTX *in vivo* after DIDS (0.25 mmol/L) treatment (n = 20). (F) Schematic representation of tumors in nude mice treated under different conditions (PTX, HGC-27-EVs/PTX, HGC-27R-EVs/PTX, and HGC-27R+DIDS-EVs/PTX). (G) The weight of subcutaneously transplanted tumors in the four groups. (H) IHC analysis of cleaved caspase-3, Ki-67, LC3B, VDAC1, and P-gp in subcutaneous transplanted tumors from four groups. DIDS, 4,4′-diisothiocyanatostilbene-2,2′-disulfonic acid; EV, extracellular vesicle; IHC, Immunohistochemistry; PTX, paclitaxel; P-gp, P-glycoprotein; VDAC1,voltage-dependent anion channel protein 1.

Intercellular transfer of EV-derived VDAC1 protein confers PTX resistance *in vivo*

Xenograft tumor model was established through subcutaneous injection of HGC-27 cells into nude mice to investigate the role of PTX-resistant cell-derived EV *in vivo*. The nude mice were randomly divided into the following six experimental groups when tumor volumes reached approximately 50 mm^3: PBS; PTX (10 mg/kg); HGC-27R-EVs-shNC (50 μg); HGC-27R-EVs-shVDAC1; HGC-27R-EVs-shNC/PTX; and HGC-27R-EVs-shVDAC1/PTX (**Figure 6A**). At the endpoint of the experiment, no significant differences in tumor volume or weight were observed between the HGC-27R-EVs-shNC and HGC-27R-EVs-shNC/PTX groups, indicating that EV-mediated chemoresistance reduced the sensitivity of GC cells to PTX treatment *in vivo*. Moreover, the volume and weight of subcutaneously transplanted tumors in the HGC-27R-EVs-shVDAC1/PTX group were significantly lower than those in the HGC-27R-EVs-shNC/PTX group (**Figures 6B, C and S3B**). In the absence of EV-derived VDAC1 protein, the ability of EVs to spread resistance was weakened, suggesting that inhibition of the EV-derived VDAC1 protein increases the sensitivity of GC to PTX, which was consistent with the *in vitro* results. In addition, IHC analysis revealed that the P-gp, LC3B, VDAC1, and Ki-67 levels were highest in the HGC-27R-EVs-shNC and HGC-27R-EVs-shNC/PTX groups with no significant difference, suggesting that the transmission of PTX resistance by EV-derived VDAC1 protein through autophagy led to a reduction in the sensitivity of GC cells to PTX (**Figures 6D and S3C**). Furthermore, the level of cleaved caspase-3 was highest in the HGC-27R-EVs-shVDAC1/PTX group. In summary, these results suggested that intercellular transfer of EV-derived VDAC1 protein induced PTX resistance in GC cells, a process that involves autophagy activation.

DIDS, a VDAC1 oligomerization inhibitor, was used to surmount PTX resistance in GC cells with high VDAC1 expression to evaluate the clinical treatment significance of targeting EV-derived VDAC1 protein in GC[43]. First, AutodockVina 1.2.2 was used to confirm the binding affinities and modes of interaction between DIDS and VDAC1 through visible hydrogen bonds and strong electrostatic interactions (**Figure S3D**). In addition, *in vitro* experiments showed that DIDS significantly reduced VDAC1 expression in both PTX-resistant GC cells and the EVs (**Figure S3E**). Then, EVs derived from GC cells were labeled with DiR dye and injected *via* the tail vein into nude mice (**Figure 6E**). EVs accumulated mainly in the liver, as the results shown in **Figure S3F**. Moreover, the results of *in vivo* experiments showed that nude mice treated with HGC-27R+DIDS-EVs/PTX exhibited significantly decreased tumor volume and weight compared to mice receiving HGC-27R-EVs/PTX (**Figures 6F, G and S3G**). Moreover, IHC staining showed the P-gp, LC3B, VDAC1, and Ki-67 levels were reduced, while the cleaved caspase-3 levels were higher in the

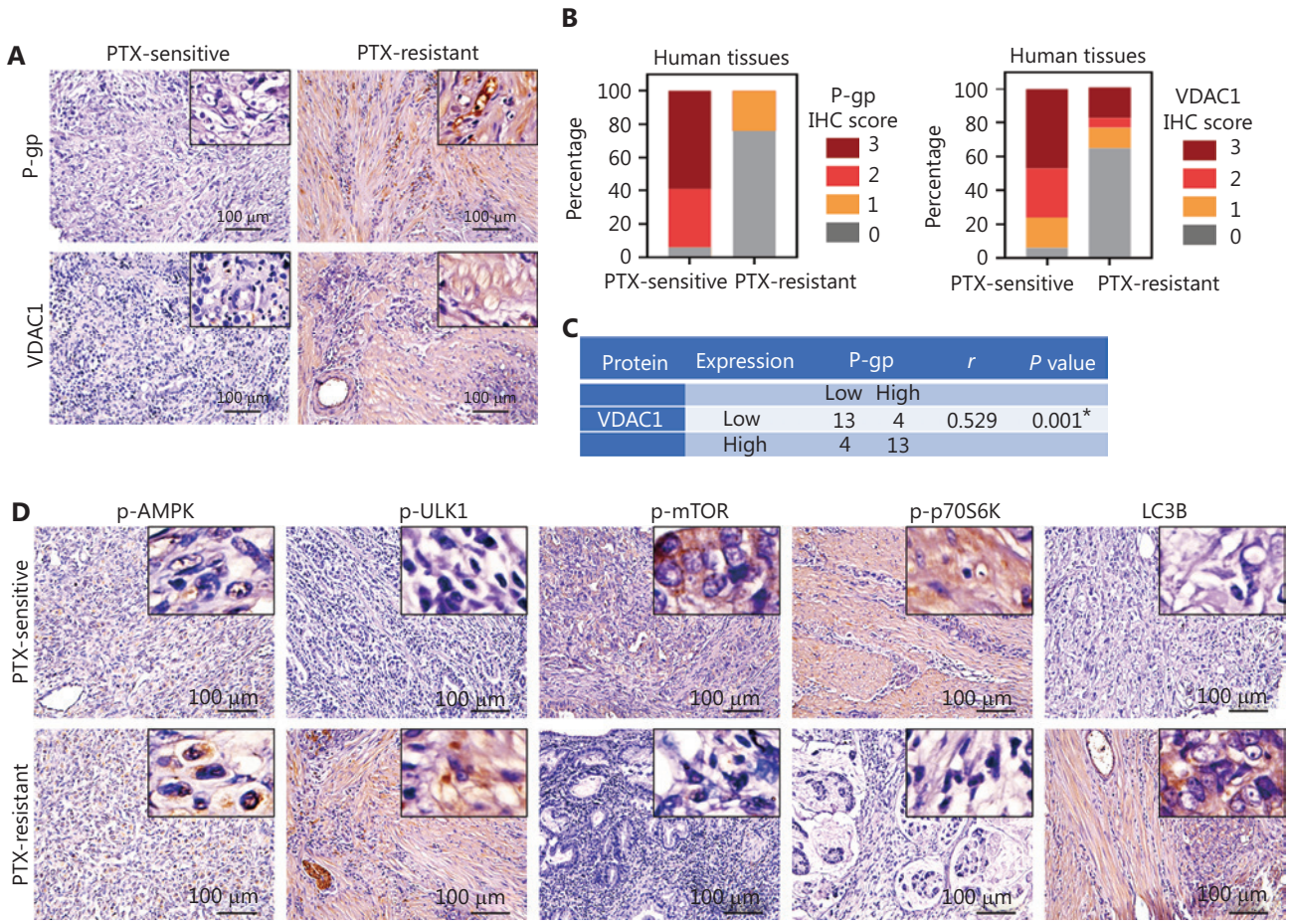


Figure 7 Continued

HGC-27R+DIDS-EVs/PTX group compared to the HGC-27R-EVs/PTX treatment group (**Figure S4**). Collectively, these results suggested that EV-derived VDAC1 protein is a potential therapeutic target for averting PTX resistance of GC and a specific inhibitor of VDAC1, such as DIDS, might serve as a component of combination therapy to overcome PTX resistance.

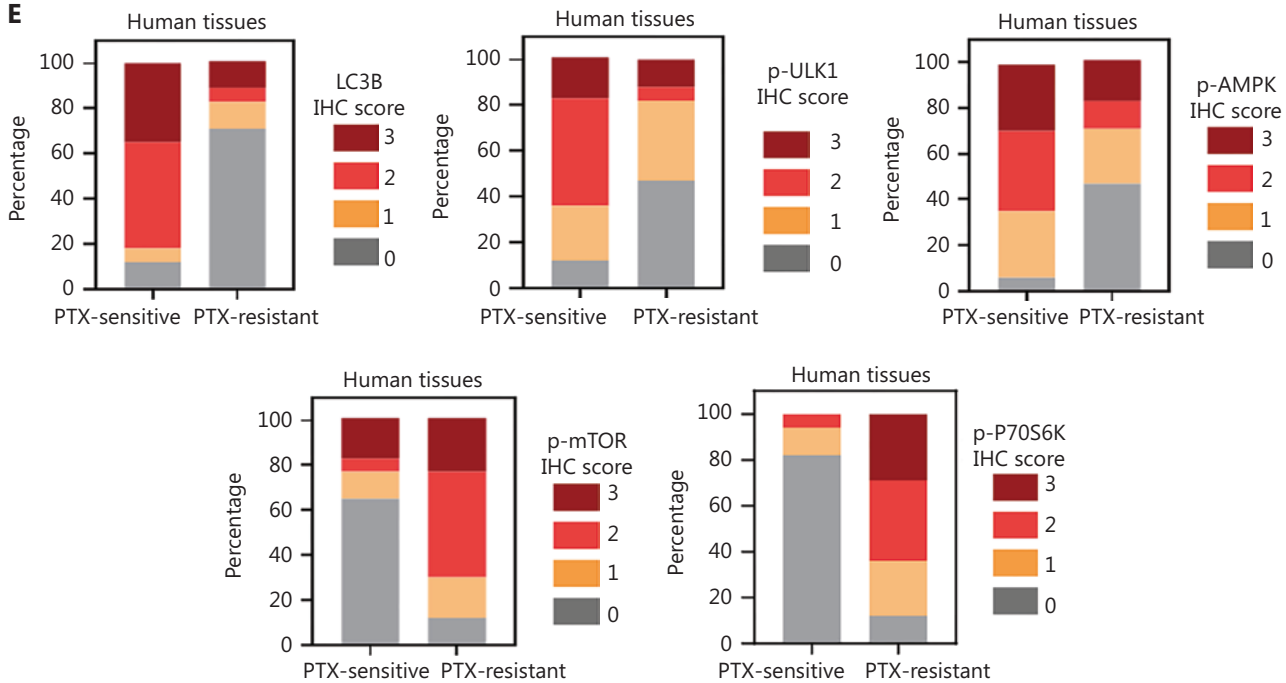
Clinical significance of VDAC1 in GC

Thirty-four pathologic sections from GC patients (17 PTX-sensitive and 17 PTX-resistant samples) were analyzed to assess VDAC1 expression and its association with autophagy markers, aiming to further explore the clinical relevance of VDAC1 in GC treatment. The VDAC1 and P-gp proteins were highly expressed in PTX-resistant tissues compared to PTX-sensitive tissues (**Figure 7A**) and were positively correlated (r = 0.529, P = 0.001; **Figure 7B, C**), which were consistent with our previous experiments. This discovery implied that the presence of VDAC1 protein has a crucial role in the development of PTX resistance in GC cells. Furthermore, a parallel increase in LC3B expression was correlated with elevated VDAC1 levels (r = 0.529, P = 0.001; **Figure 7D, E, F**), indicating that VDAC1 may drive chemoresistance *via* autophagy activation. In addition, PTX-resistant GC samples exhibited enhanced AMPK (r = 0.354, P = 0.040) and ULK1 phosphorylation (r = 0.415, P = 0.015) while decreased p-p70S6K (r = −0.415, P = 0.015) and p-mTOR (r = −0.529, P = 0.001) compared to PTX-sensitive GC samples (**Figure 7D, E, F**). Together, these findings confirmed that the VDAC1 protein facilitates the development of PTX resistance in GC cells primarily *via* the AMPK/mTOR autophagy pathway.

Discussion

PTX is recognized as a second-line treatment option for advanced GC patients[44,45]. Although PTX exerts significant cytotoxic effects in the treatment of advanced GC, a considerable proportion of patients develop acquired resistance to PTX during administration, ultimately leading to treatment

E



F

Protein	Expression	VDAC1		*r*	*P* value
		Low	High	0.415	0.015*
p-ULK1	Low	13	6		
	High	4	11		
		Low	High	0.354	0.040*
p-AMPK	Low	12	6		
	High	5	11		
		Low	High	–0.529	0.001*
p-mTOR	Low	4	13		
	High	13	4		
		Low	High	–0.415	0.015*
p-p70S6K	Low	6	13		
	High	11	4		
		Low	High	0.529	0.001*
LC3B	Low	13	4		
	High	4	13		

Figure 7 Clinical significance of VDAC1 in GC. (A) Representative IHC images of VDAC1 and P-gp expression in PTX-sensitive and -resistant patients (n = 34). (B) Statistical comparison of VDAC1 and P-gp expression between 17 PTX-sensitive and 17 PTX-resistant patients. (C) Correlation analysis of VDAC1 and P-gp expression in 17 PTX-sensitive *vs.* 17 PTX-resistant patients. (D) Representative IHC images of LC3B, p-AMPK, p-mTOR, p-p70S6K, and p-ULK1 expression in PTX-sensitive and -resistant patients (n = 34). (E) Statistical comparison of LC3B, p-AMPK, p-mTOR, p-p70S6K, and p-ULK1 expression between 17 PTX-sensitive and 17 PTX-resistant patients. (F) Correlation analysis of LC3B, p-AMPK, p-mTOR, p-p70S6K, p-ULK1, and VDAC1 expression in 17 PTX-sensitive *vs.* 17 PTX-resistant patients. AMPK, Adenosine 5′-monophosphate (AMP)-activated protein kinase; EV, extracellular vesicle; GC, gastric cancer; IHC, Immunohistochemistry; mTOR, mammalian target of Rapamycin; P-gp, P-glycoprotein; p70S6K, p70 ribosomal protein S6 kinase; PTX, paclitaxel; ULK1, unc-51 like autophagy activating kinase 1; VDAC1, voltage-dependent anion channel protein 1.

failure[46,47]. EVs have recently emerged as influential regulators of cancer drug resistance with growing evidence demonstrating their crucial role in mediating resistance transmission[48,49]. Thus, identifying which substances are contained in EVs that transmit drug resistance and developing appropriate therapeutic measures are among the most effective ways to overcome drug resistance.

The role of EVs as mediators of intercellular communication is widely acknowledged. Emerging evidence indicates that certain proteins encapsulated within EVs selectively transport cargo to recipient cells and modulate biological processes[50-52]. For example, P-gp, multidrug resistance-associated protein 1 (MRP1), and lamin B receptor (LBR) can be transferred to drug-sensitive cells *via* EVs, thereby conferring chemotherapy resistance[53,54]. However, the mechanisms underlying EV-mediated drug resistance remain largely uninvestigated, presenting a challenging task in the identification of novel targets[55]. Hence, an assessment was performed on EVs released by PTX-resistant cells and it was shown that EVs derived from PTX-resistant cells are internalized by PTX-sensitive cells within hours, inducing PTX resistance. The elimination of EVs from the conditioned media of drug-resistant cells did not result in the development of PTX resistance in PTX-sensitive cells, at least to some extent. Subsequent proteomic profiling revealed that the VDAC1 localized within EVs serves as a critical modulator of PTX resistance mechanisms. Furthermore, previous studies revealed that DIDS suppresses VDAC1 expression[56]. The data herein extend these observations by revealing that DIDS effectively inhibits EV-mediated VDAC1 release and enhances PTX sensitivity in GC. These results established EV-derived VDAC1 protein as a novel therapeutic target for chemoresistant GC and identify DIDS as a potential agent for reversing PTX resistance.

Autophagy is the evolutionarily conserved circulating process of engulfing excess or damaged cytoplasmic material into vesicles and transporting the cytoplasmic material

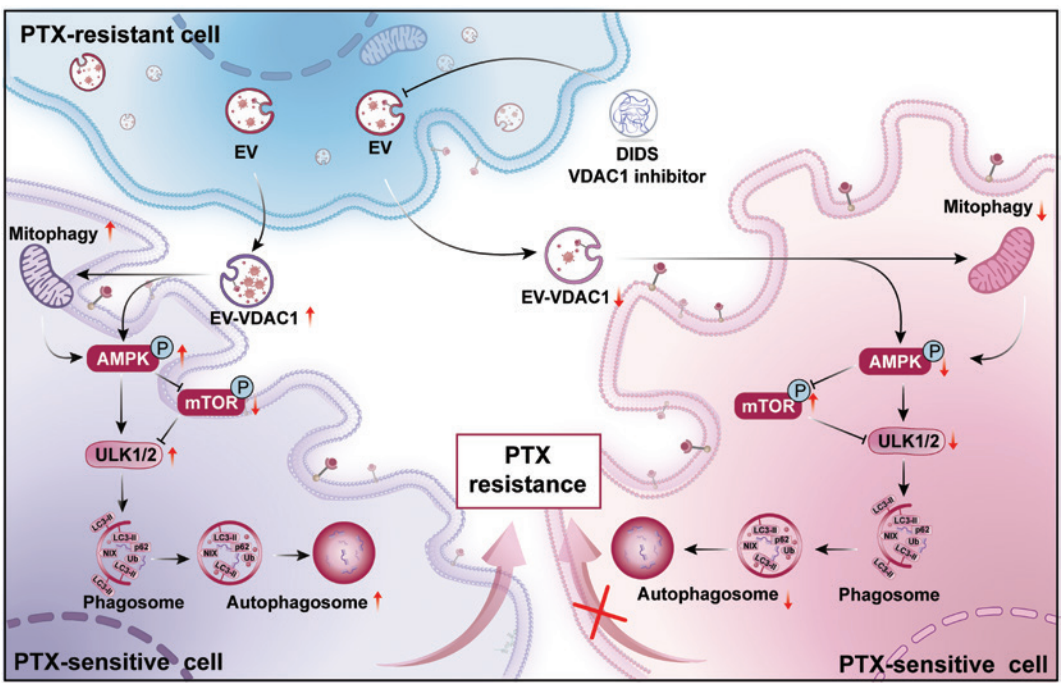


Figure 8 Proposed model for the role of EV-derived VDAC1 in mediating PTX resistance in GC. (Left) VDAC1 is packaged into extracellular vesicles (EVs) in PTX-resistant GC cells. These EVs are internalized by PTX-sensitive cells, where VDAC1 activates the AMPK signaling pathway. Activated AMPK inhibits mTOR, leading to ULK1 activation, which subsequently induces autophagy and mitophagy. This process confers PTX resistance to recipient cells. (Right) The VDAC1 inhibitor, DIDS, blocks the function of EV-derived VDAC1 protein in recipient cells. This process prevents AMPK activation, maintains mTOR activity, and suppresses ULK1. Consequently, inhibition of autophagy and mitophagy restores cellular sensitivity to PTX. This finding highlights the therapeutic potential of inhibiting EV-mediated VDAC1 transfer. AMPK, adenosine 5′-monophosphate (AMP)-activated protein kinase; DIDS, 4,4′-diisothiocyanatostilbene-2,2′-disulfonic acid; EV, extracellular vesicle; GC, gastric cancer; mTOR, mammalian target of rapamycin; PTX, paclitaxel; ULK1, Unc-51-like autophagy activating kinase 1; VDAC1, voltage-dependent anion channel protein 1.

to lysosomes for degradation, thereby fulfilling metabolic requirements and facilitating the renewal of some cellular organelles[57,58]. Mitophagy is the selective degradation of damaged or excessive mitochondria by an autophagic pathway[59,60]. In the current study when PTX-sensitive GC cells were treated with EV-derived VDAC1 protein, a significant elevation in the quantity of both mitophagosomes and autophagosomes was detected, indicating the involvement of general autophagy and mitophagy in this process. Currently, autophagy and mitophagy are widely recognized as protective mechanisms during cancer development through their role in establishing and sustaining tumor multidrug resistance[61,62]. The current study showed that VDAC1 protein encapsulated in EVs facilitates the development of chemoresistance in cancer cells *via* a dual-pathway regulatory mechanism that concurrently modulates general autophagy and activates mitophagy. VDAC1, as one of the most abundant integral membrane proteins on the outer mitochondrial membrane, has a critical role in cellular energy exchange[63]. The results showed that abnormalities in VDAC1 indirectly disrupted ATP transmembrane transport and impaired the $\Delta\psi m$ stability, directly demonstrating that VDAC1 dysfunction blocks energy exchange between mitochondria and the cytosol. ATP can directly or indirectly regulate AMPK activity[64]. Consequently, elevated VDAC1 significantly activated autophagy, including general autophagy and mitophagy, in PTX-resistant GC cells, primarily through the AMPK/mTOR pathway-mediated upregulation of autophagy-related genes. Moreover, upon internalization of EV-derived VDAC1 protein by PTX-sensitive GC cells, these cells acquired a PTX-resistant phenotype manifested through AMPK activation and concomitant mTOR signaling pathway inactivation. Collectively, these findings identified EV-derived VDAC1 transfer as a novel therapeutic target for overcoming PTX resistance in GC, highlighting the dual role in modulating both mitochondrial homeostasis and autophagic flux.

This study focused on the overall regulatory mechanisms of the AMPK/mTOR pathway. However, the current study did not delve deeply into distinguishing the specific functional differences between ULK1-dependent and -independent pathways, which indeed constitutes a current limitation. Corollary studies will use ULK1 knockout models and kinase-dead mutants, combined with dual-pathway inhibitors targeting both AMPK and mTOR. This approach will delineate the relative contributions of ULK1-dependent *versus* -independent pathways under specific physiologic conditions, as well as elucidate the cell type-specificity of the crosstalk regulation between these pathways. Furthermore, the enrichment of VDAC1 in EVs is more likely to be mediated through an ESCRT-independent pathway. However, the precise mechanism remains elusive and necessitates further experimental validation.

Conclusion

In summary, VDAC1-derived EVs were shown to have a novel role in mediating PTX resistance (**Figure 8**). The results suggested that the excessive general autophagy and mitophagy induced by EV-derived VDAC1 protein might be the primary contributing factor for drug resistance induction in GC cells in response to PTX treatment. Implying EV-derived VDAC1 protein as a potential target against GC and highlighting that general autophagy and mitophagy could hold promise as therapeutic targets for cancer. It is notable that DIDS effectively inhibits the release of EV-derived VDAC1 protein and enhances the sensitivity of GC cells to PTX to reverse drug resistance.

Grant support

This research was supported by Hebei Natural Science Foundation (Grant No. H2022206299) and the National Natural Science Foundation of China (Grant Nos. 82374090, U21A20415, and 82472636).

Conflict of interest statement

No potential conflicts of interest are disclosed.

Author contributions

Conceived and designed the analysis: Guogui Sun, Yumin Wang, Lianmei Zhao.
Collected the data: Yuqing Wang, Yang Wen, Kexin Li, Cong Zhang.
Contributed data or analysis tools: Zhe Zhang, Hongquan Wang.
Performed the analysis: Yanna Bi, Sisi Wei.
Wrote the paper: Yanna Bi, Sisi Wei.

Data availability statement

All data generated or analyzed during this study are included in the published article. The mass spectrometry proteomics data have been deposited to the ProteomeXchange Consortium (https://proteomecentral.proteomexchange.org) *via* the iProX partner repository with the dataset identifier, PXD056923[65,66].

References

1. Cao W, Chen HD, Yu YW, Li N, Chen WQ. Changing profiles of cancer burden worldwide and in China: a secondary analysis of the global cancer statistics 2020. Chin Med J. 2021; 134: 783-91.

2. Li Q, Xia C, Li H, Yan X, Yang F, Cao M, et al. Disparities in 36 cancers across 185 countries: secondary analysis of global cancer statistics. Front Med. 2024; 18: 911-20.
3. Nakayama I, Takahari D, Shimozaki K, Chin K, Wakatsuki T, Ogura M, et al. Clinical progress in inoperable or recurrent advanced gastric cancer treatment from 1004 single institute experiences between 2007 and 2018. Oncologist. 2022; 27: e506-17.
4. Kang BW, Kwon OK, Chung HY, Yu W, Kim JG. Taxanes in the treatment of advanced gastric cancer. Molecules. 2016; 21: 651.
5. Al-Batran SE, Van Cutsem E, Oh SC, Bodoky G, Shimada Y, Hironaka S, et al. Quality-of-life and performance status results from the phase III RAINBOW study of ramucirumab plus paclitaxel versus placebo plus paclitaxel in patients with previously treated gastric or gastroesophageal junction adenocarcinoma. Ann Oncol. 2016; 27: 673-9.
6. Lordick F. Gastrointestinal cancer: Salvage chemotherapy in gastric cancer – more than a straw? Nat Rev Clin Oncol. 2012; 9: 312-3.
7. Ho SWT, Sheng T, Xing M, Ooi WF, Xu C, Sundar R, et al. Regulatory enhancer profiling of mesenchymal-type gastric cancer reveals subtype-specific epigenomic landscapes and targetable vulnerabilities. Gut. 2022; 72: 226-41.
8. Cheng L, Hill AF. Therapeutically harnessing extracellular vesicles. Nat Rev Drug Discov. 2022; 21: 379-99.
9. Tsai MJ, Hsu YL, Kuo PL. Circulating extracellular vesicles in human disease. N Engl J Med. 2018; 379: 2179-80.
10. Xavier CPR, Belisario DC, Rebelo R, Assaraf YG, Giovannetti E, Kopecka J, et al. The role of extracellular vesicles in the transfer of drug resistance competences to cancer cells. Drug Resist Updat. 2022; 62: 100833.
11. Morimoto M, Maishi N, Hida K. Acquisition of drug resistance in endothelial cells by tumor-derived extracellular vesicles and cancer progression. Cancer Drug Resist. 2024; 7: 1.
12. Ming-Kun C, Zi-Xian C, Mao-Ping C, Hong C, Zhuang-Fei C, Shan-Chao Z. Engineered extracellular vesicles: a new approach for targeted therapy of tumors and overcoming drug resistance. Cancer Commun (Lond). 2024; 44: 205-25.
13. Słomka A, Wang B, Mocan T, Horhat A, Willms AG, Schmidt-Wolf IGH, et al. Extracellular vesicles and circulating tumour cells – complementary liquid biopsies or standalone concepts? Theranostics. 2022; 12: 5836-55.
14. van Niel G, D'Angelo G, Raposo G. Shedding light on the cell biology of extracellular vesicles. Nat Rev Mol Cell Biol. 2018; 19: 213-28.
15. Tashakori N, Armanfar M, Mashhadi A, Mohammed AT, Karim MM, Hussein AHA, et al. Deciphering the role of exosomal non-coding RNA (ncRNA) in drug resistance of gastrointestinal tumors; an updated review. Cell Biochem Biophys. 2024; 82: 609-21.
16. Marima R, Basera A, Miya T, Damane BP, Kandhavelu J, Mirza S, et al. Exosomal long non-coding RNAs in cancer: interplay, modulation, and therapeutic avenues. Noncoding RNA Res. 2024; 9: 887-900.
17. Dong P, Xiong Y, Yue J, J B Hanley S, Kobayashi N, Todo Y, et al. Exploring lncRNA-mediated regulatory networks in endometrial cancer cells and the tumor microenvironment: advances and challenges. Cancers (Basel). 2019; 11: 234.
18. Zhou W, Fong MY, Min Y, Somlo G, Liu L, Palomares MR, et al. Cancer-secreted miR-105 destroys vascular endothelial barriers to promote metastasis. Cancer Cell. 2014; 25: 501-15.
19. Liu SJ, Dang HX, Lim DA, Feng FY, Maher CA. Long noncoding RNAs in cancer metastasis. Nat Rev Cancer. 2021; 21: 446-60.
20. Wang Y, Zhang Y, Li Z, Wei S, Chi X, Yan X, et al. Combination of size-exclusion chromatography and ion exchange adsorption for improving the proteomic analysis of plasma-derived extracellular vesicles. Proteomics. 2023; 23: e2200364.
21. Raposo G, Stoorvogel W. Extracellular vesicles: exosomes, microvesicles, and friends. J Cell Biol. 2013; 200: 373-83.
22. Tian Y, Ma L, Gong M, Su G, Zhu S, Zhang W, et al. Protein profiling and sizing of extracellular vesicles from colorectal cancer patients via flow cytometry. ACS Nano. 2018; 12: 671-80.
23. Wei S, Sun S, Zhou X, Zhang C, Li X, Dai S, et al. SNHG5 inhibits the progression of EMT through the ubiquitin-degradation of MTA2 in oesophageal cancer. Carcinogenesis. 2021; 42: 315-26.
24. Wei S, Li X, Wang J, Wang Y, Zhang C, Dai S, et al. Outer membrane vesicles secreted by *Helicobacter pylori* transmitting gastric pathogenic virulence factors. ACS Omega. 2021; 7: 240-58.
25. Trajkovic K, Hsu C, Chiantia S, Rajendran L, Wenzel D, Wieland F, et al. Ceramide triggers budding of exosome vesicles into multivesicular endosomes. Science. 2008; 319: 1244-7.
26. Wang X, Hao Y, Chen J, Ding P, Lv X, Zhou D, et al. Nuclear complement C3b promotes paclitaxel resistance by assembling the SIN3A/HDAC1/2 complex in non-small cell lung cancer. Cell Death Dis. 2023; 14: 351.
27. Cao L, Zhou Y, Li X, Lin S, Tan Z, Guan F. Integrating transcriptomics, proteomics, glycomics and glycoproteomics to characterize paclitaxel resistance in breast cancer cells. J Proteomics. 2021; 243: 104266.
28. Liu Z, Luo Q, Guo C. Bim and VDAC1 are hierarchically essential for mitochondrial ATF2 mediated cell death. Cancer Cell Int. 2015; 15: 34.
29. Yang Z, Liu H, Song Y, Gao N, Gao P, Hui Y, et al. Luteolin enhances drug chemosensitivity by downregulating the FAK/PI3K/AKT pathway in paclitaxel-resistant esophageal squamous cell carcinoma. Int J Mol Med. 2024; 54: 77.
30. Bayrhuber M, Meins T, Habeck M, Becker S, Giller K, Villinger S, et al. Structure of the human voltage-dependent anion channel. Proc Natl Acad Sci U S A. 2008; 105: 15370-5.
31. Keinan N, Tyomkin D, Shoshan-Barmatz V. Oligomerization of the mitochondrial protein voltage-dependent anion channel is coupled to the induction of apoptosis. Mol Cell Biol. 2010; 30: 5698-709.
32. Geula S, Naveed H, Liang J, Shoshan-Barmatz V. Structure-based analysis of VDAC1 protein: defining oligomer contact sites. J Biol Chem. 2012; 287: 2179-90.
33. Nielsen RB, Larsen BS, Holm R, Pijpers I, Snoeys J, Nielsen UG, et al. Increased bioavailability of a P-gp substrate: co-release of etoposide and zosuquidar from amorphous solid dispersions. Int J Pharm. 2023; 642: 123094.

34. St George M, Ayoub AT, Banerjee A, Churchill CDM, Winter P, Klobukowski M, et al. Designing and testing of novel taxanes to probe the highly complex mechanisms by which taxanes bind to microtubules and cause cytotoxicity to cancer cells. PLoS One. 2015; 10: e0129168.
35. Xiao M, Benoit A, Hasmim M, Duhem C, Vogin G, Berchem G, et al. Targeting cytoprotective autophagy to enhance anticancer therapies. Front Oncol. 2021; 11: 626309.
36. Zhang S-F, Wang X-Y, Fu Z-Q, Peng Q-H, Zhang J-Y, Ye F, et al. TXNDC17 promotes paclitaxel resistance via inducing autophagy in ovarian cancer. Autophagy. 2015; 11: 225-38.
37. Zhou C, Zhong W, Zhou J, Sheng F, Fang Z, Wei Y, et al. Monitoring autophagic flux by an improved tandem fluorescent-tagged LC3 (mTagRFP-mWasabi-LC3) reveals that high-dose rapamycin impairs autophagic flux in cancer cells. Autophagy. 2012; 8: 1215-26.
38. Xiao B, Goh J-Y, Xiao L, Xian H, Lim K-L, Liou Y-C. Reactive oxygen species trigger Parkin/PINK1 pathway-dependent mitophagy by inducing mitochondrial recruitment of Parkin. J Biol Chem. 2017; 292: 16697-708.
39. Chen Y, Qian J, Ding P, Wang W, Li X, Tang X, et al. Elevated SFXN2 limits mitochondrial autophagy and increases iron-mediated energy production to promote multiple myeloma cell proliferation. Cell Death Dis. 2022; 13: 822.
40. Wang N, Wang B, Maswikiti EP, Yu Y, Song K, Ma C, et al. AMPK-a key factor in crosstalk between tumor cell energy metabolism and immune microenvironment? Cell Death Discov. 2024; 10: 237.
41. Steinberg GR, Hardie DG. New insights into activation and function of the AMPK. Nat Rev Mol Cell Biol. 2023; 24: 255-72.
42. Inoki K, Kim J, Guan K-L. AMPK and mTOR in cellular energy homeostasis and drug targets. Annu Rev Pharmacol Toxicol. 2012; 52: 381-400.
43. Zhu X, Luo L, Xiong Y, Jiang N, Wang Y, Lv Y, et al. VDAC1 oligomerization may enhance DDP-induced hepatocyte apoptosis by exacerbating oxidative stress and mitochondrial DNA damage. FEBS Open Bio. 2022; 12: 516-22.
44. Wilke H, Muro K, Van Cutsem E, Oh S-C, Bodoky G, Shimada Y, et al. Ramucirumab plus paclitaxel versus placebo plus paclitaxel in patients with previously treated advanced gastric or gastro-oesophageal junction adenocarcinoma (RAINBOW): a double-blind, randomised phase 3 trial. Lancet Oncol. 2014; 15: 1224-35.
45. Zhao Q, Wu T, Tang C, Li J, Wu M, Wu J, et al. Biomimetic nanocrystals co-deliver paclitaxel and small-molecule LF3 for ferroptosis-combined chemotherapy for gastric cancer. Colloids Surf B: Biointerfaces. 2025; 251: 114586.
46. Katsaounis P, Kotsakis A, Kentepozidis N, Polyzos A, Bakogeorgos M, Koinis F, et al. Nab-paclitaxel as second-line treatment in advanced gastric cancer: a multicenter phase II study of the Hellenic Oncology Research Group. Ann Gastroenterol. 2018; 31: 65-70.
47. Hironaka S, Ueda S, Yasui H, Nishina T, Tsuda M, Tsumura T, et al. Randomized, open-label, phase III study comparing irinotecan with paclitaxel in patients with advanced gastric cancer without severe peritoneal metastasis after failure of prior combination chemotherapy using fluoropyrimidine plus platinum: WJOG 4007 trial. J Clin Oncol. 2013; 31: 4438-44.
48. Camussi G, Deregibus MC, Bruno S, Grange C, Fonsato V, Tetta C. Exosome/microvesicle-mediated epigenetic reprogramming of cells. Am J Cancer Res. 2010; 1: 98-110.
49. Jena BC, Mandal M. The emerging roles of exosomes in anti-cancer drug resistance and tumor progression: An insight towards tumor-microenvironment interaction. Biochim Biophys Acta Rev Cancer. 2021; 1875: 188488.
50. Jafari N, Llevenes P, Denis GV. Exosomes as novel biomarkers in metabolic disease and obesity-related cancers. Nat Rev Endocrinol. 2022; 18: 327-8.
51. Han Q-F, Li W-J, Hu K-S, Gao J, Zhai W-L, Yang J-H, et al. Exosome biogenesis: machinery, regulation, and therapeutic implications in cancer. Mol Cancer. 2022; 21: 207.
52. Havryliuk V, Wojtowicz K, Gagat M, Żuryń A. Exosome-mediated mechanisms of drug resistance in lung cancer: molecular mechanisms and therapeutic strategies. Cell Physiol Biochem. 2025; 59: 358-74.
53. Han M, Gu Y, Lu P, Li J, Cao H, Li X, et al. Exosome-mediated lncRNA AFAP1-AS1 promotes trastuzumab resistance through binding with AUF1 and activating ERBB2 translation. Mol Cancer. 2020; 19: 26.
54. Li X, Li X, Michael A-F, Liu H, Li R, Liu J, et al. Investigation of the attenuation effect of licorice on the toxicity of rhubarb using a P-gp lipid raft bioaffinity chromatography. J Ethnopharmacol. 2025; 349: 119929.
55. Wu S, Luo M, To K, Zhang J, Su C, Zhang H, et al. Abstract 1101: Intercellular transfer of exosomal wild type EGFR triggers osimertinib resistance in non-small cell lung cancer. Cancer Res. 2021; 81: 1101.
56. Chen H, Gao W, Yang Y, Guo S, Wang H, Wang W, et al. Inhibition of VDAC1 prevents Ca^{2+}-mediated oxidative stress and apoptosis induced by 5-aminolevulinic acid mediated sonodynamic therapy in THP-1 macrophages. Apoptosis. 2014; 19: 1712-26.
57. Vargas JNS, Hamasaki M, Kawabata T, Youle RJ, Yoshimori T. The mechanisms and roles of selective autophagy in mammals. Nat Rev Mol Cell Biol. 2023; 24: 167-85.
58. Harper JW, Ordureau A, Heo J-M. Building and decoding ubiquitin chains for mitophagy. Nat Rev Mol Cell Biol. 2018; 19: 93-108.
59. Kulikov AV, Luchkina EA, Gogvadze V, Zhivotovsky B. Mitophagy: link to cancer development and therapy. Biochem Biophys Res Commun. 2017; 482: 432-9.
60. Lemasters JJ. Selective mitochondrial autophagy, or mitophagy, as a targeted defense against oxidative stress, mitochondrial dysfunction, and aging. Rejuvenation Res. 2005; 8: 3-5.
61. Hwang ST, Kim C, Lee JH, Chinnathambi A, Alharbi SA, Shair OHM, et al. Cycloastragenol can negate constitutive STAT3 activation and promote paclitaxel-induced apoptosis in human gastric cancer cells. Phytomedicine. 2019; 59: 152907.
62. Mukherjee S, Bhatti GK, Chhabra R, Reddy PH, Bhatti JS. Targeting mitochondria as a potential therapeutic strategy against chemoresistance in cancer. Biomed Pharmacother. 2023; 160: 114398.

63. Shteinfer-Kuzmine A, Santhanam M, Shoshan-Barmatz V. VDAC1-based peptides as potential modulators of VDAC1 interactions with its partners and as a therapeutic for cancer, NASH, and diabetes. Biomolecules. 2024; 14: 1139.
64. Ke R, Xu Q, Li C, Luo L, Huang D. Mechanisms of AMPK in the maintenance of ATP balance during energy metabolism. Cell Biol Int. 2018; 42: 384-92.
65. Ma J, Chen T, Wu S, Yang C, Bai M, Shu K, et al. iProX: an integrated proteome resource. Nucleic Acids Res. 2019; 47: D1211-7.
66. Chen T, Ma J, Liu Y, Chen Z, Xiao N, Lu Y, et al. iProX in 2021: connecting proteomics data sharing with big data. Nucleic Acids Res. 2022; 50: D1522-7.

Cite this article as: Bi Y, Wei S, Zhang Z, Wang Y, Wen Y, Wang H, et al. VDAC1 protein derived from extracellular vesicles promotes paclitaxel resistance in gastric cancer through autophagy and mitophagy. Cancer Biol Med. 2026; 23: 252-275. doi: 10.20892/j.issn.2095-3941.2025.0360